# Advanced Physics- Based Modeling of Discrete Clutter and Diffuse Reverberation in the Littoral Environment

**STTR Phase I - Topic N03-T011**
**1 July 2003 – 2 February 2004**

**Peter Neumann and Gregory Muncill**
**Planning Systems Incorporated**
**12030 Sunrise Valley Drive**
**Suite 400, Reston Plaza 1**
**Reston, VA 20191-3453**
**(540) 552-5102 (Phone)**
**pneumann@plansys.com (Email)**

**Charles Holland**
**Penn State University**
**Applied Research Lab**
**P.O. Box 30**
**State College, PA 16804-0030**

**Kevin LePage**
**Naval Research Lab**
**Washington, DC 20375-5320**

**Contract Number: N00014-03-M-0266**

**Phase I STTR Summary Report**

**UNCLASSIFIED**

**Issuing Agency:**

**Office of Naval Research**
**Attn: James McEachern, Code 321US**
**Ballston Tower One**
**800 North Quincy Street**
**Arlington, VA 22217-5660**

# Report Documentation Page

*Form Approved*
*OMB No. 0704-0188*



| 1. REPORT DATE | 2. REPORT TYPE | 3. DATES COVERED |
|---|---|---|
| **02 FEB 2004** | **Summary** | **01 Jul 2003 - 02 Feb 2004** |

4. TITLE AND SUBTITLE
**Advanced Physics-Based Modeling of Discrete Cluter and Diffuse Reverberation in the Littoral Environment**

5a. CONTRACT NUMBER
**N00014-03-M-0266**

5b. GRANT NUMBER

5c. PROGRAM ELEMENT NUMBER

6. AUTHOR(S)
**Peter Neumann (PSI), Charles Holland (ARL/PSU), Kevin LePage (NRL-DC), Greg Muncill (PSI)**

5d. PROJECT NUMBER

5e. TASK NUMBER

5f. WORK UNIT NUMBER

7. PERFORMING ORGANIZATION NAME(S) AND ADDRESS(ES)
**Planning Systems Incorporated 12030 Sunrise Valley Drive Suite 400, Reston Plaza 1 Reston, VA 20191-3453 Penn State University Applied Research Lab P. O. Box 30 State College, PA 16804-0030 Naval Research Lab Washington, D.C. 20375-05320**

8. PERFORMING ORGANIZATION REPORT NUMBER

9. SPONSORING/MONITORING AGENCY NAME(S) AND ADDRESS(ES)
**Office of Naval Research Attn: James McEachern, Code 321 SS Ballston Tower One 800 North Quincy Street Arlington, VA 22217-5660**

10. SPONSOR/MONITOR'S ACRONYM(S)

11. SPONSOR/MONITOR'S REPORT NUMBER(S)

12. DISTRIBUTION/AVAILABILITY STATEMENT
**Approved for public release, distribution unlimited**

13. SUPPLEMENTARY NOTES
**The original document contains color images.**

14. ABSTRACT
**The results of this Phase I STTR show that a number of the currently identified mechanisms responsible for geoclutter are understood and can be modeled. Charles Holland presents a summary of the observed target-like returns from mud volcanoes. The summary of existing diffuse reverberation models shows the approximations made in currently used models. The research by Kevin LePage presents a capability to directly model broadband time series using a coherent summation of narrowband predictions. This capability applied to both diffuse reverberation and recently to discrete clutter is recommended for continued development and transition into a configuration managed simulation product. Applications of this proposed simulation product have been identified within both the AEER and LAMP program in a meeting with representatives of these programs. At the end of the Phase I base program, the goals of a physics based simulation of a broadband time series including the effects of both discrete clutter and diffuse reverberation for frequencies below 5 KHz are attainable. The proposed Phase I option will allow the development of this simulation package to be continued in the time before the Phase II funding is in place.**

15. SUBJECT TERMS
**STTR Report, Discrete clutter, diffuse reverberation, littoral environments, high-fidelity modeling, geoclutter, boundary characterization, scatter mechanisms**

| 16. SECURITY CLASSIFICATION OF: | | | 17. LIMITATION OF ABSTRACT | 18. NUMBER OF PAGES | 19a. NAME OF RESPONSIBLE PERSON |
|---|---|---|---|---|---|
| a. REPORT | b. ABSTRACT | c. THIS PAGE | | | |
| **unclassified** | **unclassified** | **unclassified** | **UU** | **69** | |

**Standard Form 298 (Rev. 8-98)**
Prescribed by ANSI Std Z39-18

# Table of Contents

# List of Figures

## Executive Summary

The goals of the Phase I STTR tasks were to identify the key discrete clutter mechanisms identified in the research to date and to report on the current state-of-the-art in diffuse reverberation and discrete clutter modeling. This report summarizes the results from the key researchers on this Phase I STTR and presents our plan for transitioning these results into a broadband time series simulator.

The challenges for active ASW sonar systems include the problems of discrete clutter and diffuse bottom reverberation. Diffuse bottom reverberation, at present, is the better understood of the two with a variety of approaches to modeling that will be covered later in this report. The problem of understanding and modeling discrete clutter is now coming to the forefront as the Navy operates their active sonar systems more often in littoral areas.

The work of Charles Holland, presented in the first section of this report, shows the extent to which the mechanisms causing discrete clutter are now understood. An overview is presented for the case of mud volcanoes which have caused target like returns in several experiments conducted in the Malta Plateau. This research has shown that these mud volcanoes can produce target like returns with a size scale comparable to that of a target ($O(10^1\text{-}10^2)$ m) with target strengths from 15 to 30 dB. These mud volcanoes appear to be persistent over decadal time scales. A more general presentation of other clutter mechanisms from the sea surface, ocean volume, seabed and anthropogenic features is also included in this first section of the report.

The second section of the report covers the current state of diffuse reverberation and discrete clutter modeling. Beginning with the two Navy standard performance prediction models, ASPM (Acoustic System Performance Model) and CASS (Comprehensive Acoustic System Simulation), the overview presents the capabilities of each model with a focus on its potential use in the problem of broadband time series simulation. The third model presented is a simulation package called SST (Sonar Simulation Toolset) developed and maintained by APL/UW. SST is a time series simulator that is commonly applied at torpedo frequencies and is used as a simulator for some of the larger weapons simulations. The research work of Chris Harrison and Kevin LePage close this section. The conclusion of this evaluation is that none of the existing performance prediction model or simulation packages present a practical starting point for the proposed Phase II development of a physics based, broadband time series simulation of discrete clutter and diffuse reverberation. The reasons for not beginning the proposed Phase II work with ASPM, CASS or SST are provided in this section of the report. It should be noted in this introduction, that the SST package provides a great many elements of the proposed simulation product but the challenges involved in adding a new propagation loss model, scattering kernels and mechanisms for discrete clutter appeared to be beyond the scope of what could be completed under the Phase II limits of time and funding. In addition, after meeting with representatives of the EER program and the LAMP program, some of the perceived advantages of SST (e.g., developed for UNIX in Fortran and C/C++) were not necessary for their applications.

Kevin LePage closes the section of this report that covers the Phase I findings with a summary of his current modeling work on discrete clutter. His approach to simulation of broadband

waveforms (without resorting to the computationally intensive technique of Fourier synthesis of narrowband results) is extremely promising and is proposed for further development in Phase II. This approach also will satisfy the requirements of the EER and LAMP programs (see section titled "Requirements for Broadband Time Series Modeling from the EER and LAMP Programs").

One additional modeling capability that was requested by representatives of the EER program was an ability to simulate the frequency spread that occurs due to interaction with the sea surface and near surface bubble clouds. This modeling capability is outside of the scope of the initial Phase I proposal but will be proposed as a Phase II option task to be conducted at or near the end of the Phase II base program period of performance. OAML approval or at least an independent V&V of the completed product before its adoption by these programs was also mentioned as an important consideration.

At the end of the Phase I base program, the goals of a physics based simulation of a broadband time series including the effects of both discrete clutter and diffuse reverberation for frequencies below 5 KHz are attainable. The proposed Phase I option will allow the development of this simulation package to be continued in the time before the Phase II funding is in place. The interaction with the EER and LAMP program has already resulted in a better understanding of those programs' requirements and has resulted in a proposed broadening of the capabilities of the simulation package to include frequency spread due to sea surface interaction. This report summarize the phase I findings, interaction with the EER and LAMP programs, phase II plans and phase III commercialization opportunities.

## Phase I Findings

The Phase I findings are divided by the tasks described in the Phase I STTR proposal. The first section is written by Charles Holland (ARL/PSU) and covers the research he has performed and summarized on the various discrete clutter mechanisms observed in experiments. The second section is written by Peter Neumann (PSI) and Kevin LePage (NRL-DC) summarizes the reverberation models currently available and the current research on reverberation modeling. The third section is written by Kevin LePage and summarizes his current work on clutter modeling.

### Base Program Task 1 – Clutter Analyses

The performance of active Navy ASW sonar systems in littoral environments is often limited by strong discrete clutter and diffuse bottom reverberation. Discrete clutter, in particular, (which leads to high false alarm rates) is widely viewed as one of the most important limiting environmental factors in the operation of active ASW sonar systems in littoral areas. Discrete clutter, tends to be nearly ubiquitous, (i.e., found in nearly every region where Navy sonars operate) but its characteristics have been difficult to predict. One of the primary reasons that prediction has been difficult is that the underlying mechanisms giving rise to the clutter are largely unknown.

Analyses of two clutter mechanisms observed in the Straits of Sicily are discussed in some detail in the following section entitled "Seabed Clutter Analyses from the Malta Plateau." This analysis includes identification of the mechanism as well as the estimation of parameters that would be

needed to model the clutter events. The section titled "Clutter Mechanisms Summary" provides a general summary (i.e., not tied to any particular geographic location) of potential clutter mechanisms from the sea surface, ocean volume, seabed and anthropogenic features.

***Seabed Clutter Analyses from the Malta Plateau***

Geoclutter (target-like returns from features of geologic origin) may be classified in two broad categories, (1) clutter produced from bathymetric features, e.g., outcropping rock or ridge structures and (2) clutter produced from features that are at or below the seabed interface. The latter category is the main focus of this analysis, and is of considerable importance since it may occur in areas where the seabed is otherwise relatively flat and featureless.

A series of four experiments from 1998-2002 were conducted in the Straits of Sicily (Malta Plateau, see Figure 1) to develop techniques that quantitatively describe sediment geoacoustic properties and to identify seabed features that produce geoclutter. One of the principal seabed mechanisms leading to sonar clutter on the Malta Plateau appears to be gas. The gas is frequently associated with truncated conical structures of order 10 m in diameter believed to be mud volcanoes (Holland et al., 2003). The mud volcano structure may rise several meters above the surrounding seabed or be partially, or fully buried below the water-sediment interface. For active mud volcanoes (at or above the seafloor) gas is expelled into the water column and the presence of the gas plume is a potential mechanism for clutter (only "geoclutter" in the sense that its origins are geologic). Some of the mud volcanoes are buried several meters under a fine-grained silty-clay that has a lower sound speed than that in the water column (i.e., there is no critical angle and very low compressional wave attenuation). Since the sediment above the mud volcanoes is nearly acoustically transparent, these sub-bottom features are a potential source of geoclutter.

Mud volcanoes form due to the rise of fluidized sediments along a fault or on top of a seafloor-piercing shale diapir. They may occur in areas of earthquake activity, originate from thick clay beds, usually erupt along fault lines and often bubble methane gas, and sometimes oil. Although there is a considerable body of literature pertaining to sub-aerial (on-land) mud volcanoes, submarine mud volcanoes are a relatively new research field. They are known to occur both in deep and shallow water and in a variety of geologic settings, including the abyssal parts of inland seas, active margins, continental slopes of passive margins and continental shelves (Milkov, 2000).

A summary of the geophysical survey results is provided in the section titled "Geophysical Survey results," addressing both large-scale bathymetric features and gassy sediments. In the section titled "Clutter Observations," acoustic observations of the clutter from long-range reverberation are presented and the seabed features corresponding to the clutter events are described. Acoustic reverberation and reflection data are analyzed in the section titled "Temporal and spectral characteristics of the clutter" to examine several hypotheses about the mechanisms that lead to the observed clutter. An estimate of the bubble size distribution of both the active and buried mud volcanoes are also provided, which would be required for a physics-based clutter model.

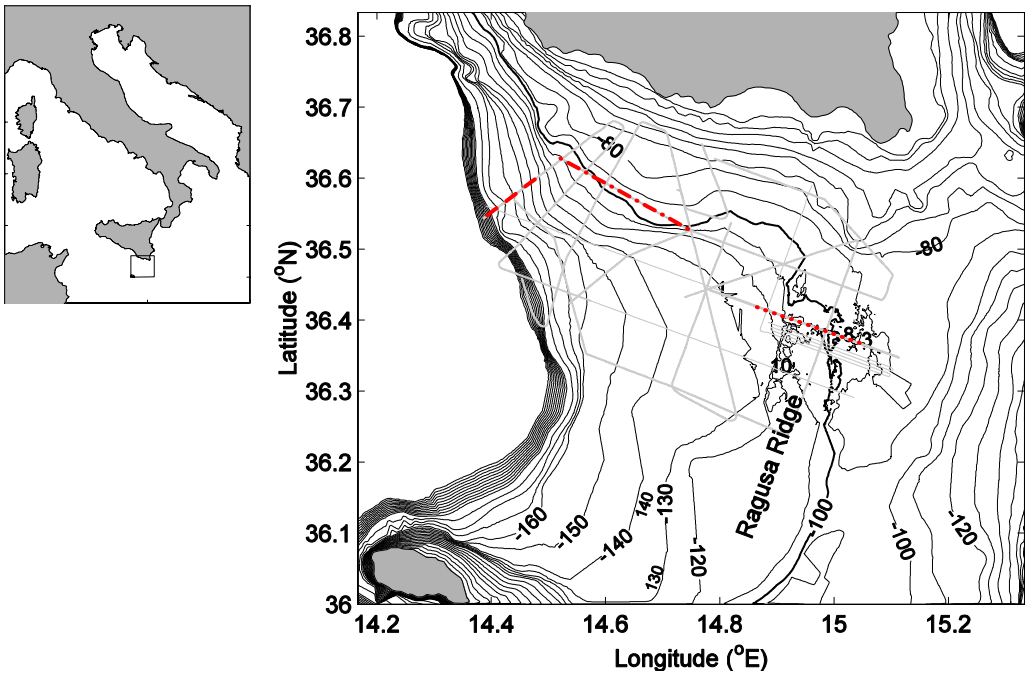


**Figure 1: Malta Plateau study area between Sicily (to the north) and Maltese island of Gozo (to the south). Seismic reflection survey, tracks are indicated by grey lines with depths in meters. Specific seismic reflection lines of interest are indicated by the dashed line (see Figure 2), the dotted line (Figure 4) and the dash-dotted line (Figure 9).**

*Geophysical Survey results*

A variety of geophysical equipment was employed during the experiments. Two different boomers were employed for seabed reflection profiling: an EG&G model before 1999 and a Geoacoustics Uniboomer (operated at 280 Joules) thereafter. The pulse rate and tow depths for both boomers was one pulse per second and approximately 0.4 m respectively. In 2002, an Edgetech DF-100 side-scan sonar and 216D sub-bottom profiler housed in a single towed vehicle was towed 10-20 meters above the bottom. The chirp was set at the 2-10 kHz band yielding a vertical resolution of approximately 0.10 m. The beamwidth was approximately 20 degrees with a pulse rate of 0.250 second.

*Large-scale Bathymetric Features*

The Malta Plateau occupies the northern edge of the North African passive continental margin and is a submerged section of the Hyblean Plateau of mainland Sicily (Max et al., 1993). A discussion of the geology of this area, along with seismic reflection data can be found in (Max et al., 1993 and Osler and Algan, 1999). The region (see Figure 1) is divided by the Ragusa Ridge, roughly defined by depths shallower than 110 m, which forms a spine approximately 20 km wide between Sicily and Malta. The area west of the ridge is blanketed with a silty-clay sediment, which thickens from about 1 m at 150 m water depth to about 8 m at the 100 m water depth contour.

The most prominent bathymetric feature on the Malta Plateau is the Ragusa Ridge. High resolution bathymetry collected in SCARAB98, MAPEX2000 and Boundary2000 (see Figure 2) show that the western rim of the Ragusa Ridge is approximately linear, trending south southwest and sinuous in depth. This prominent bathymetric feature (the western rim) generates both clutter and interference (i.e., scattering that is not "target-like" in its temporal statistics but is of high enough level to mask potential targets). Clutter is also generated from rock outcrops east of the rim (see Figure 3) especially where gaps in the rim exist.

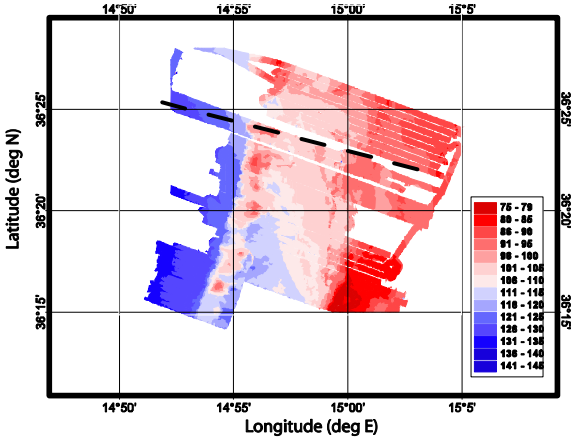


**Figure 2: Multibeam bathymetry collected on the Ragusa Ridge, depths are in meters. The dashed line shows the track line for the seismic reflection data shown in Figure 3.**

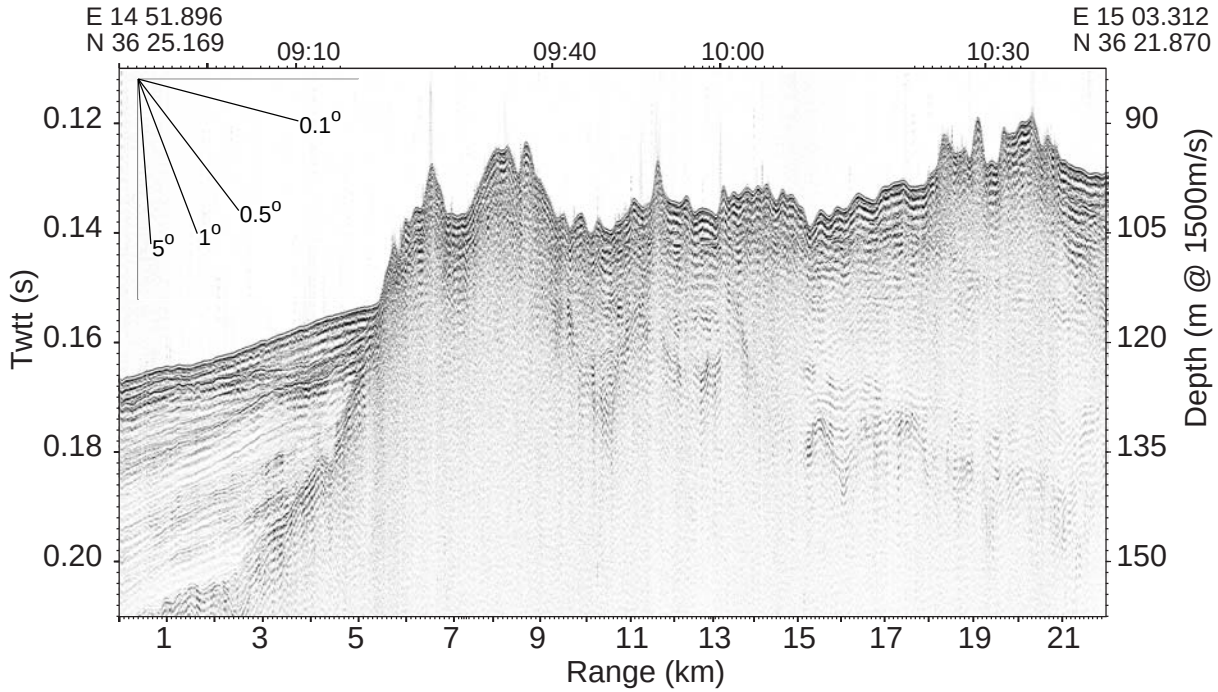


**Figure 3: Seismic reflection data showing rocky outcrops on the ridge and layered sediments to the west of the Ragusa Ridge.**

*Mud volcano observations*

Mud volcanoes were first detected (but not identified) during a seismic reflection survey, where they appeared as cone-like features about 4 meters high on the seabed (Figure 4, at 5 and 5.8 km range). A later survey track was conducted over these features with a sidescan sonar. The sidescan data (see Figure 5) reveals two scales of features: clusters of truncated cylinders roughly 10 m in diameter rising up to 4 meters above the seafloor, and surrounding these, patches of high scattering strength approximately 50 m in diameter. The diffuse shadow behind the features appears to be caused by attenuation due to gas rising into the water column. The reason that the seismic reflection data (Figure 4) show the features as cones instead of truncated cylinders as apparent from the shadows (see Figure 5), is that the source has a wide beamwidth and tends to integrate or "smear out" any large local slopes and "smear in" out-of plane scatterers. The truncated cylinders observed at this location appear to be mud volcanoes.

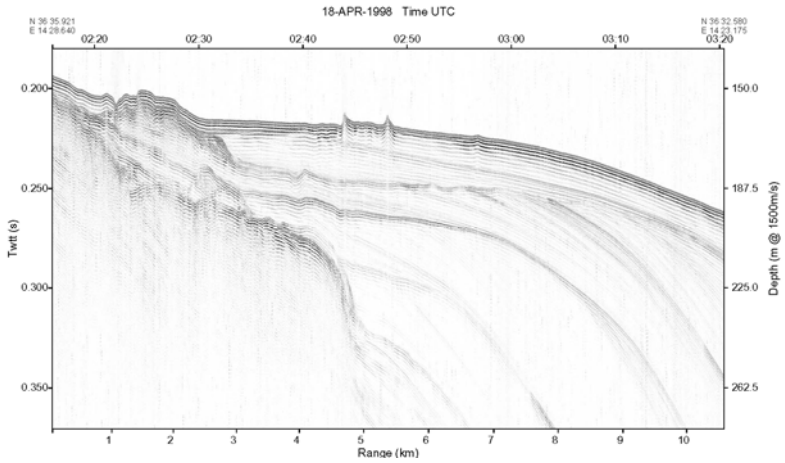


**Figure 4: Swell-filtered seismic reflection data along southwest bearing showing peculiar cone-like features (between 4 and 6 km) on the seabed. Vertical exaggeration is approximately 350:1.**

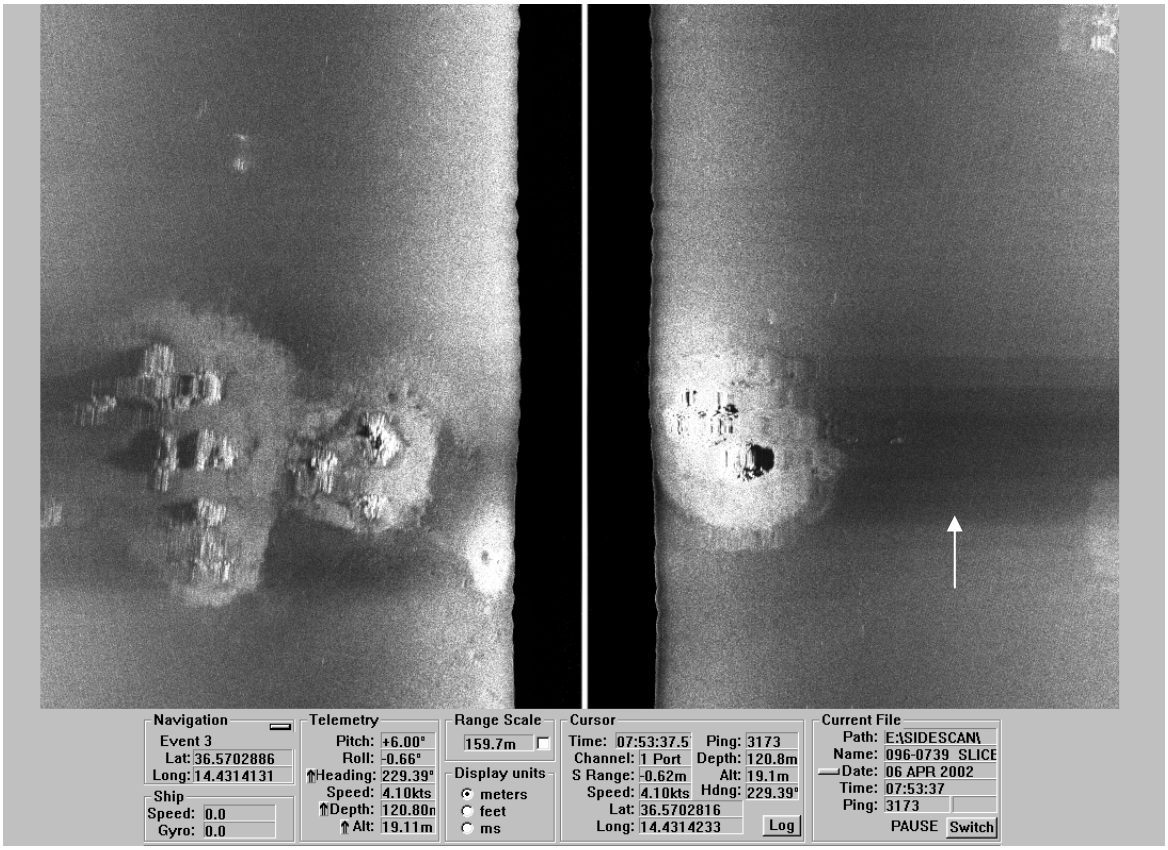


**Figure 5: Raw 100 kHz sidescan data at the northern cone-like feature of Figure 4. The scale is 320 m in cross-range with approximately square pixel size; white indicates high scattering. The arrow indicates a diffuse shadow behind the volcano that may be caused by attenuation due to venting gas.**

Figure 4 not only clearly shows the surficial volcanoes, but also several that are buried below the water-sediment interface. Following the discovery of the mud volcanoes, seismic reflection data from prior experiments were examined for evidence of mud volcanoes in other parts of the plateau. A map of the mud volcanoes (both buried and proud) known to date is shown in Figure 6. These mud volcanoes were imaged solely "by chance" in the sense that the survey was not designed to detect them, and the line spacing (of order 1 to 10 km) is much greater than the scale of the features. Thus, it is believed that there are likely to be many more submarine mud volcanoes on the Malta Plateau than are represented in this map.

*Clutter Observations*

Long-range reverberation data were acquired using impulsive SUS (Sound Undersea Signal) sources at 91 m depth. The primary advantage of the impulsive sources is the broad frequency coverage. That is, the frequency dependence of the observed clutter contains clues that may reject or support potential scattering mechanisms. The receiver was a 3-aperture nested array of 256 elements with apertures of 0.5, 1 and 2 m towed at a depth of approximately 50 m.

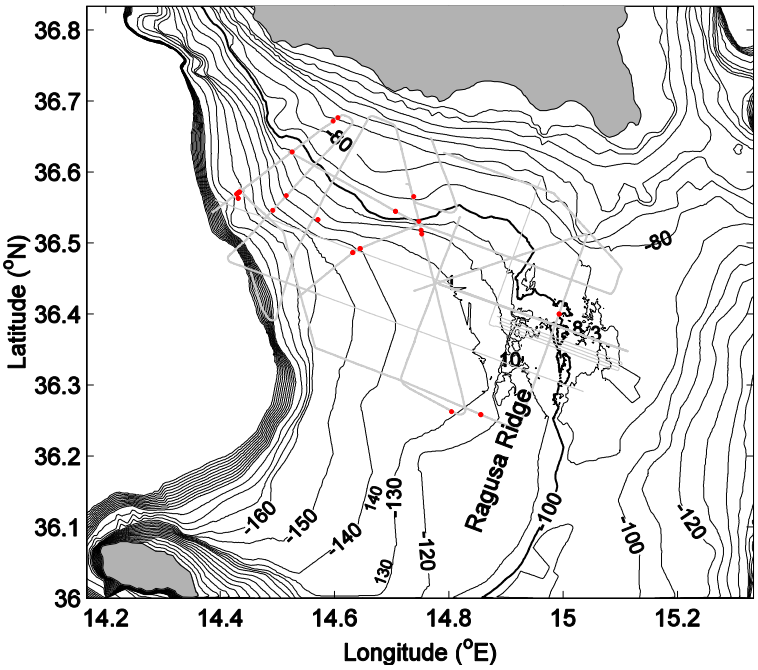


**Figure 6: Map of sub-bottom volcano locations (•) on the Malta Plateau. Seismic reflection survey lines are shown in grey.**

The reverberation data were collected near the center of the study area (see Figure 1) at 5 minute intervals. The study area (Straits of Sicily) is subject to heavy merchant ship traffic. Noise generated from nearby vessels sometimes precluded observation of clutter events of interest. During the reverberation measurements, transmission loss, XBT, seismic reflection and wind speed data (Figure 7) were collected. The low wind speed suggests that the reverberation was not dominated by sea surface scattering.

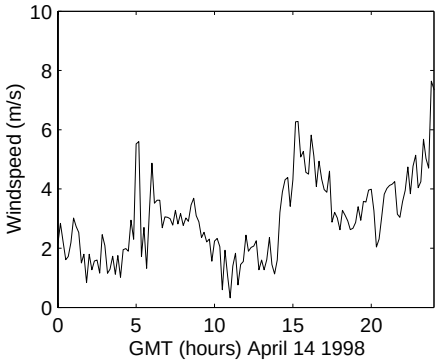


**Figure 7: April 14 wind speed measured from R/V Alliance. Reverberation experiment took place from 1000-1900 GMT.**

Broadband reverberation (100-1800 Hz) from SUS charges and a 128 element (0.5 m) aperture with Hanning shaded beams is shown in Figure 8. The data have a time variable gain correction to aid in visualization of clutter events far from the source; the units are relative decibels. The

left-right ambiguity from the array is clearly seen; the array heading is roughly west northwest. Resolving the ambiguity was performed by measuring reverberation at a variety of positions and array headings. The highest return in Figure 8 is from a nearby tanker (the noise from the tanker is visible along the entire radial). Also visible are returns that correspond to the position of 2 mud volcanoes. The southernmost mud volcano cluster is actually buried approximately 3 m sub-bottom (see Figure 9, features at approximately 4 km). It is possible that proud mud volcanoes are part of the cluster but were not imaged in the profile. It is reasonable, however, to expect that sub-bottom features may produce clutter since the sediments above the mud volcanoes are nearly acoustically transparent.[1]

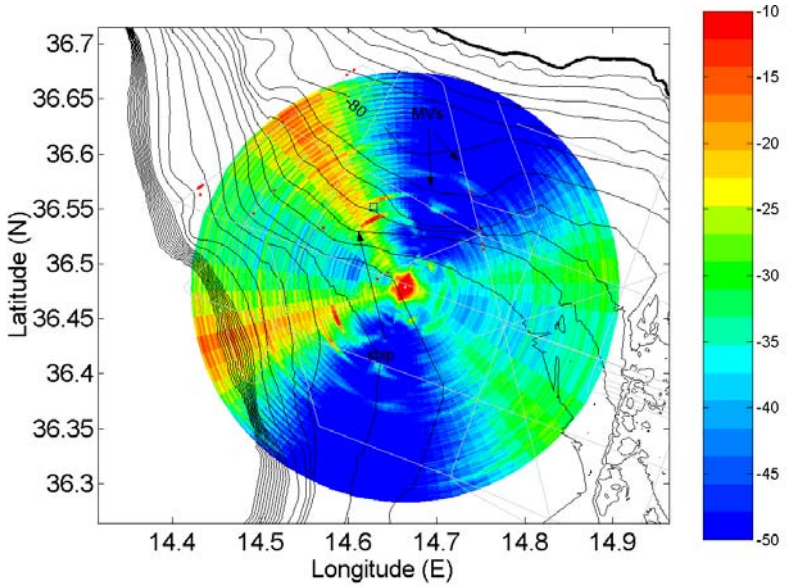


**Figure 8: Broadband reverberation (relative dB) from SUS in the Straits of Sicily. The island of Sicily is in the upper right hand corner. The data have a time variable gain. There is a left-right ambiguity in the figure around the axis of the towed array. The strong radial line to the northwest is from a ship (tanker) tending the Campo Vega oil rig (box). The reverberation return from two mud volcanoes is indicated by the arrows. The gray lines are seismic reflection survey tracks.**

[1] A sediment sound speed ratio of 0.98 and a sediment density ratio of 1.3 have been reported for this location (Holland, 2002).

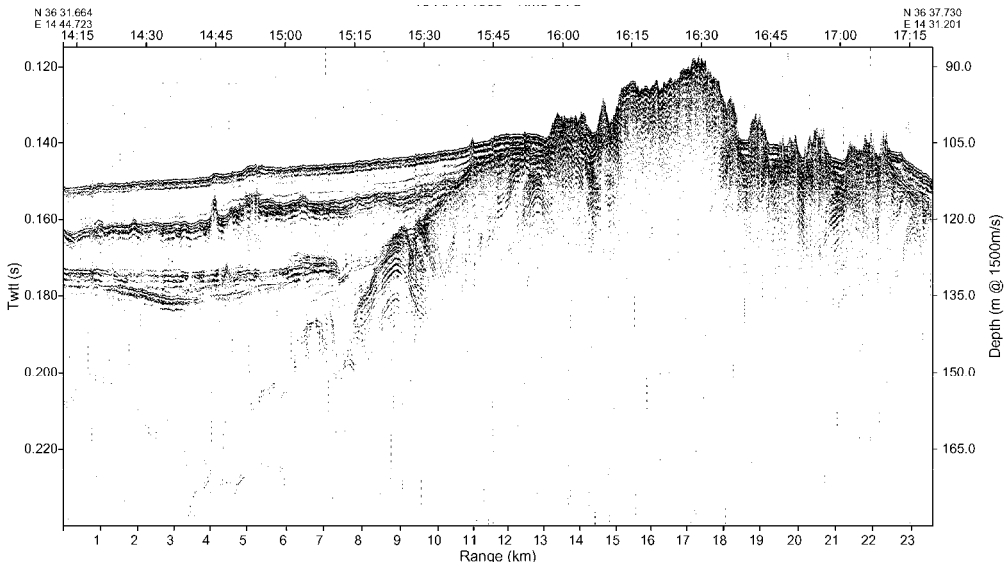


**Figure 9: Seismic reflection data along a west-northwest track showing the mud volcanoes at 4 km corresponding to the southernmost mud volcanoes shown in Figure 8. The track location is shown in Figure 1. Diffuse reverberation from the ridge (at approximately 13-20 km) would have been observed at a position approximately 36.6ºN 14.6ºE but it is masked by tanker noise.**

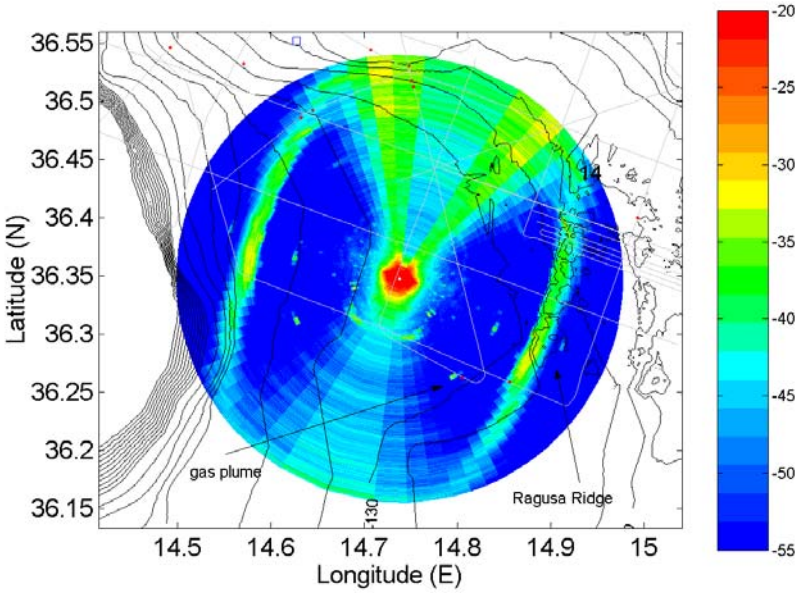


**Figure 10: Broadband (SUS) reverberation in the Straits of Sicily. The strongest return is from the Ragusa ridge. The reverberation return from a gas plume is indicated by the arrow. The clutter event at about the same amplitude to the northeast (but west of the ridge) is associated with a known wreck.**

Figure 10 shows another reverberation measurement nearer to the Ragusa ridge, the largest bathymetric feature on the shelf. There is a broad reverberation return all along the ridge and then discrete clutter events on the flat-lying sediments west of the ridge. Geophysical measurements (Figure 11) show that the southernmost clutter event is due to sediment out-gassing. The plume in the water column is about 75 m in diameter and at least 40 m in height. It is unlikely that the seismic line crossed directly over the center of the plume, thus the size estimates are lower bounds. Furthermore, if the ship track did not pass over (or within about 10 m of) the plume centre, the mud volcanoes would not be imaged in the data. Thus the absence of mud volcanoes in Figure 11 does not mean that they do not exist at this site.

*Temporal and spectral characteristics of the clutter*

There are several potential physical mechanisms for the clutter events, including scattering from the mud volcano structures (of order 10 m diameter), scattering from the gassy sediment (of order 50 m diameter) surrounding the mud volcanoes and/or scattering from the gas released into the water column. In order to examine these hypotheses, the temporal and spectral characteristics of the clutter events were analyzed.

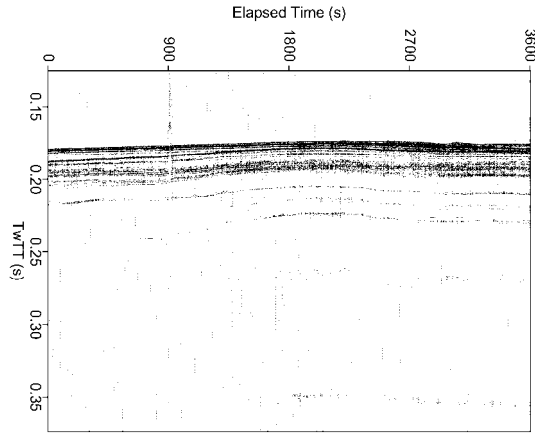


**Figure 11: Seismic reflection data over the gas plume (at 900 seconds elapsed time). The ship speed was about 4 knots so the track length (1 hour) is approximately 7.5 km. The water sediment interface is at approximately 0.18 seconds two-way travel time (TWTT); the plume is approximately 75 m in diameter. It is not clear whether the plume is associated with a mud volcano.**

*Gas plume temporal and spectral characteristics*

Multiple reverberation measurements were conducted along the track (Figure 12) 10-15 km away from the gas plume. The arrival structure of the gas plume clutter (see Figure 13 for typical return) shows time spread on the order of a few hundred milliseconds (the SUS signature is approximately 40 milliseconds between the shock and the first bubble pulse). Time spreads from

one-way propagation in the area for position of propagation measurements indicate that much of the time spread is due to propagation rather than time spread from the clutter features itself.

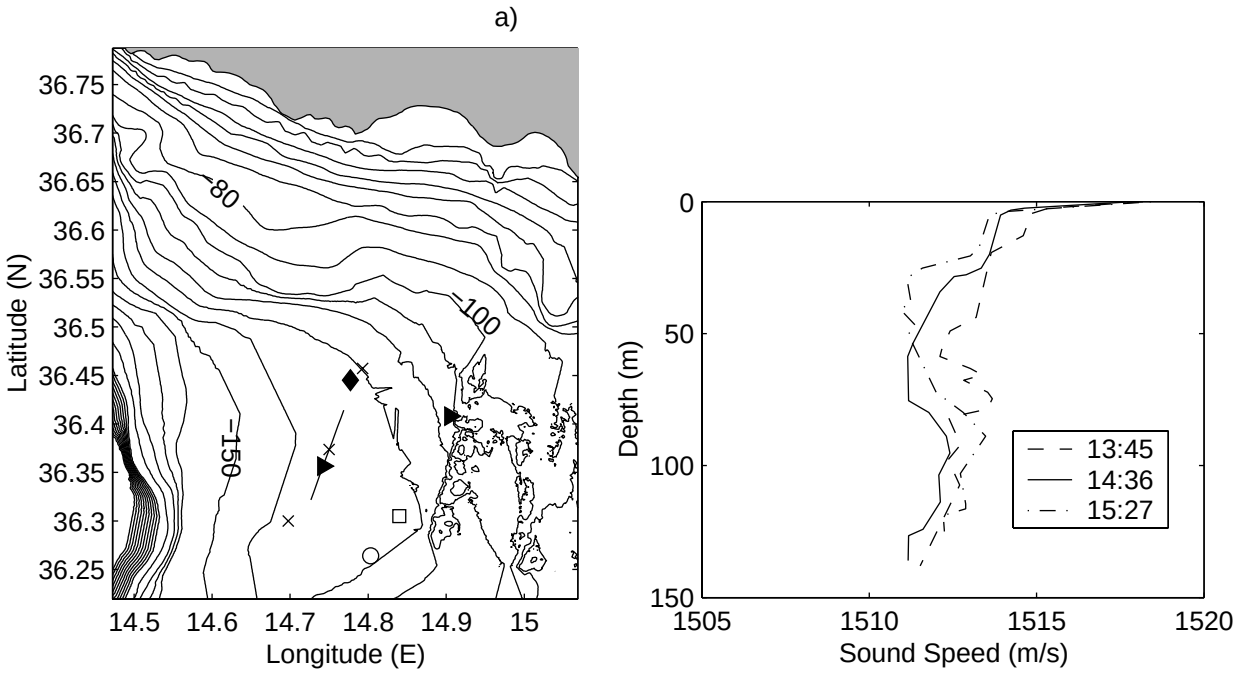


**Figure 12: a) Location of reverberation measurements (along solid line), position of receiver for propagation (♦), SUS position for downslope and upslope propagation (►), gas plume (o), wreck (□), and XBT casts (x) (depths are in meters). b) Sound speed profiles along reverberation track as a function of time (GMT). The direction of the track goes from southwest to northeast.**

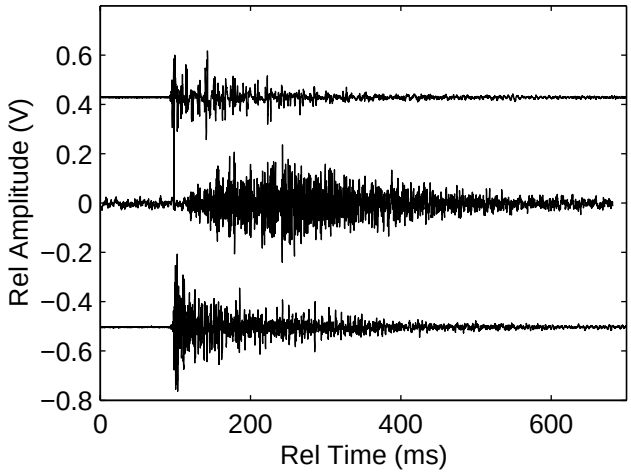


**Figure 13: Time series of plume reverberation (centered at 0 Volts) and propagation (downslope centered at –0.5 Volts and upslope centered at +0.5 Volts).**

The spectral characteristics of the clutter event (Figure 14b) were obtained by a simple sonar equation approach in order to factor out the frequency dependence of the source and the two-way propagation. The target strength (TS) of the clutter was computed with the following equation.

$$TS = RL - SL + TL_1 + TL_2$$

Here RL is the received level, SL the source level and $TL_{1,2}$ are the propagation losses to and from the scatterer. Although no propagation data were available along this particular bearing, there were upslope and downslope measurements nearby (see Figure 14a).

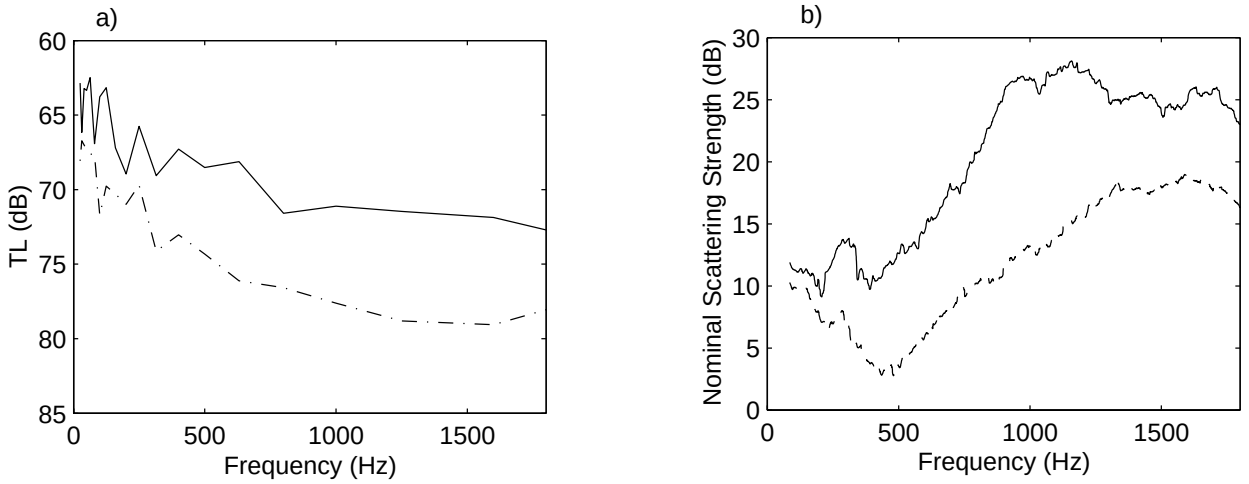


**Figure 14: a) Upslope (solid) and downslope (dash dot) propagation loss at approximately 11.8 km and 11.3 km respectively (see Figure 12a for location) , b) nominal target strength for clutter event (solid) and reverberation just before clutter event (dashed)**

In addition to the spectral characteristics of the clutter event, the spectral characteristics of the background reverberation (immediately before the clutter event) were also processed. A comparison between the two spectra provides an indication of the relative strength of the clutter event. The actual process responsible for the "background reverberation" (dashed line in Figure 14b) is diffuse scattering, thus it would normally be referenced to a scattering strength. However, the data were left as "nominal target strength" so they could be used to determine when the clutter event was significant relative to the background reverberation.

Below about 250 Hz, the clutter mechanism (solid line) is lower than or comparable to the local scattering phenomenon. However from 400-950 Hz there is a sharp increase in target strength, approximately 15 dB per octave. Above 950 Hz, scattering from the clutter event is roughly frequency independent or slowly decreases.

*Ping to ping variability of gas plume clutter*

One of the questions regarding clutter from gas-related features is temporal stability, i.e., how does the bubble size distribution vary over time? Time scales from order of seconds (ping-to-ping time scales) to order years (of importance for survey purposes) are of interest. For example it is not known whether methane ebullition occurs primarily in episodic events (perhaps

correlated with seismic activity) or whether there is a large steady state out-gassing. The reverberation measurements provide insight as to temporal fluctuations over time scales of minutes to hours. Nine observations of the clutter event were made at approximately 5 minute intervals along the solid line in Figure 12a. Variability of the sound speed profile along the track is shown in Figure 12b.

During the measurement period, the observed target strength was remarkably stable, with a standard deviation ranging from 2-3 dB (in Figure 15a). This variability includes the (unknown) variability in the source and unknown spatial/temporal variability in two-way propagation (over ranges of 9-17 km and azimuths of 130-170º). The stability of the target strength suggests that over time scales of minutes to an hour the gas bubble size distribution (or the characteristics that give rise to the clutter) is quite stable. The target strength data were averaged over a 60 Hz sliding window, the bubble pulse frequency is approximately 24 Hz. Only target strengths greater than 6 dB above the background reverberation (immediately prior to the clutter) are included in the plot. The possible dependence of target strength on azimuth (or range) was explored, but the target strength appears to be independent of both (see Figure 15d), consistent with expectations from gas plume scattering.

The TS (Figure 15a) from the plume is suggestive of two frequency regimes, one from about 250-450 Hz, where the TS is nearly constant or decreasing and the second from 450 Hz to at least 1800 Hz. Given that these two regimes may be controlled by different mechanisms, the dependence of TS on azimuth was explored separately for each frequency regime; however, neither regime evidenced a correlation between azimuth and TS.

One of the target strength observations (ping 6) is significantly below (above 800 Hz approximately 6 dB below than the mean of) the other curves (see Figure 15a,d). The difference seems significant because the standard deviation for maximum target strength at around 1 kHz is less than 1 dB for the other 8 pings. There are three obvious possibilities for the decrease in the observed target strength, a decrease in the source level, an increase in the TL along that particular bearing or a variation in the bubble size distribution. A 6 dB decrease in source level for this ping seems unlikely because for the same ping, the received level at the receiver used for transmission loss measurements shows no apparent decrease in received level. In addition, the reverberation levels at ranges just before the plume show similar levels for adjacent pings (pings 5 and 7) as ping 6 across the entire band. Thus, it appears that the TL is not the cause of the low observed plume TS on ping 6. Therefore, the most reasonable explanation is that there was a change in the characteristics of the bubble plume itself. A decrease (by approximately a factor of 4) in the number of bubbles across all radii would give a similar effect. The fact that the low frequency regime (250-450 Hz) does not show the 6 dB decrease, further suggests that this regime may be controlled by a different mechanism, perhaps scattering from gas bubbles entrained in the sediment.

The low TS of ping 6, and the fact that the TS for pings 5 minutes before and 5 minutes after are very close to the mean TS for the entire run (see Figure 15d) indicates that an independent bubble population is observed, roughly every 5 minutes. This places a lower bound on the upwelling convective rates for the plume at roughly 30 cm/s.

Finally, the stability of the target strength results in Figure 15a also suggests that the propagation is fairly stable in this zone. For each TS curve, the same TL was used. The lack of apparent correlation between the target strength and distance, suggests that the TL is reasonably constant over space and time. Clutter observations from another track collected 6 hours earlier, show TS with similar characteristics.

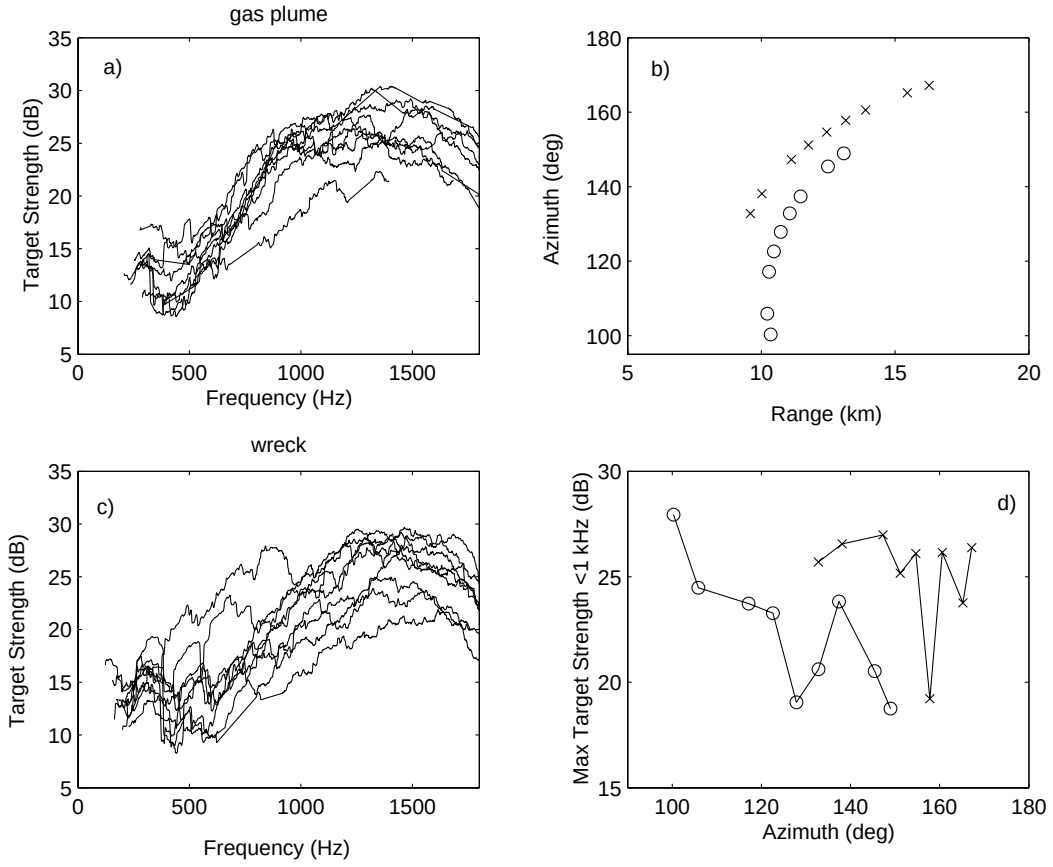


**Figure 15: Comparison of multiple observations of clutter from gas plume and wreck a) target strength data show surprisingly constant response, b) the dependence on range and azimuth from source/receiver to the gas plume(x), and wreck (o), c) target strength data from wreck show greater variability than that from the gas plume, d) Correlation between maximum target strength and azimuth for the gas plume (x) and wreck below 1000 Hz (o). As the azimuth nears 90°, the target strength rapidly increases for the wreck. There is no apparent correlation between azimuth and the target strength for the gas plume.**

Data from prior and subsequent experiments from the early 1990's to 2002 show strong clutter events at the same location. Thus, it appears that the plume and the concomitant clutter exist over decadal time scales. The data from the other trials have not been analyzed to determine if the target strength shows variability over this time scale.

*Ping to ping variability of clutter from a wreck*

The existence of a bottomed wreck nearby the gas plume (see Figure 10) affords the opportunity to compare clutter characteristics for the same set of pings. Clutter from the wreck has a similar TS across the same frequency band as that from the gas plume (Figure 15c), but shows substantially more ping-to-ping variability, especially below 1 kHz. This variability appears to be due to the inherent azimuthal response from the vessel which is lying in a roughly north/south orientation; note that the TS increases rapidly near broadside (90$^o$), see Figure 15d.

*Clutter analysis from buried mud volcanoes*

It is hypothesized that the clutter event observed in Figure 8 corresponds to scattering from a buried mud volcano. Reverberation measurements along a nearby track (see Figure 16) and transmission loss measurements (see Figure 17a) allow a similar analysis as for the gas plume and the wreck. The target strength associated with the mud volcano (Figure 17b) is distinctly different than that associated with the gas plume and the wreck inasmuch it decreases rapidly above approximately 600 Hz.

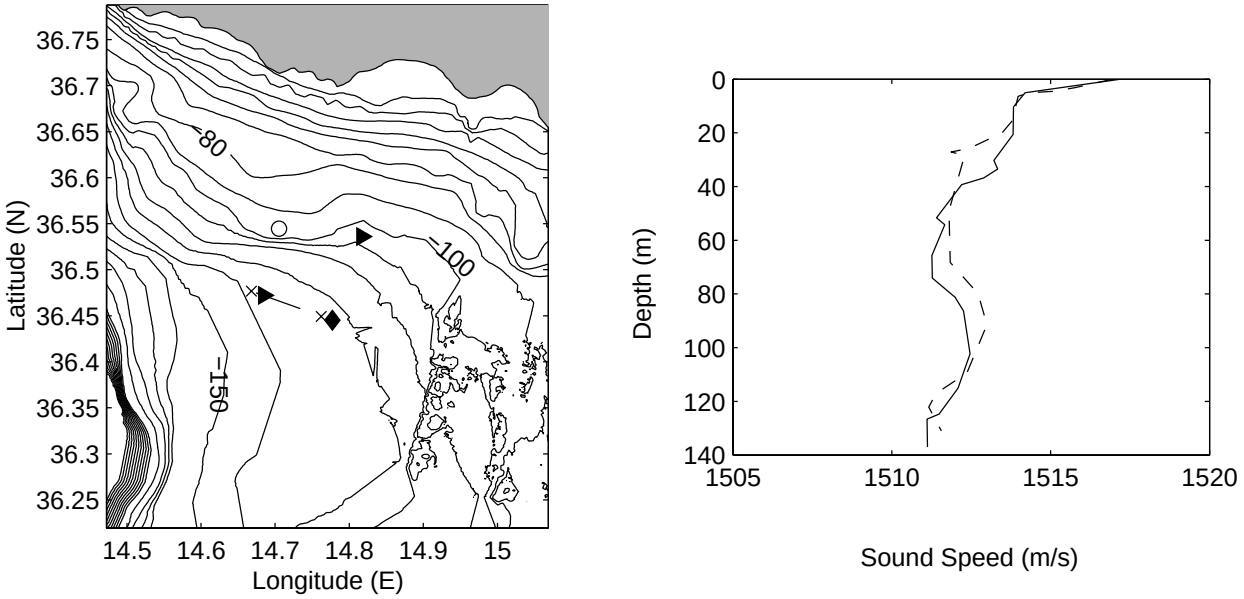


**Figure 16: a) Location of source/receiver for reverberation measurements (along solid line), position of receiver for propagation (♦), SUS position for downslope and upslope propagation (►), mud volcanoes (o), XBT casts (x), b) Sound speed profiles along reverberation track near the start of track (solid), near end of track (dashed). Track goes from east to west.**

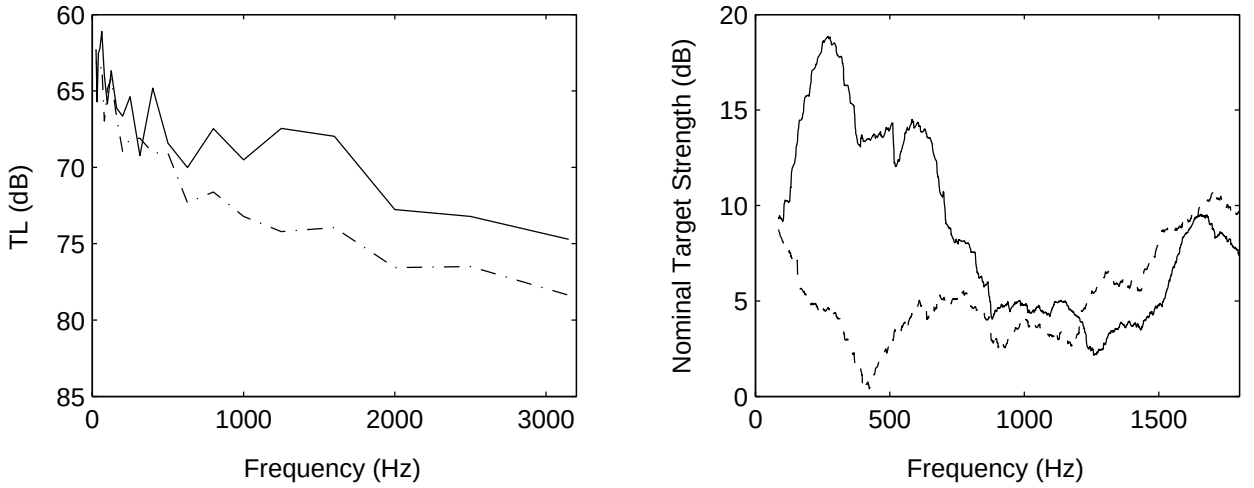


**Figure 17: a) Upslope (solid) and downslope (dash dot) propagation loss at 9.2 km for both directions (see Figure 16a for location) , b) Nominal target strength for clutter event (solid) and reverberation just before clutter event (dashed).**

Although, there is little scattering above approximately 750 Hz, the scattering below that (see Figure 18a) is similar to that from the gas plume (see Figure 15a). Both are independent of azimuth (Figure 18c), and both show a similar variability from ping to ping. The most important similarity, however, is that at low frequencies (200-500 Hz) both have a very similar target strength (mean of approximately 14 dB) and both show a gradual decrease at low frequencies (the two spectral peaks in Figure 18a are associated with two spectral peaks in the TL data and thus are not significant). Given these similarities, we speculate that the mechanism for the clutter at the low frequencies might be similar between the two sites.

Why does scattering from the mud volcano have a small contribution at frequencies above 750 Hz? One possibility is that the bubble size distribution is completely different. Another possibility is that the scattering mechanism is different, i.e., that there is no significant vented gas in the water column at the buried mud volcano site and that the clutter mechanism is associated with sediment-borne gas. Because of the relatively large attenuation in sediments (especially sediments with interstitial gas), the TS frequency dependence might be expected to be inversely proportional to frequency.

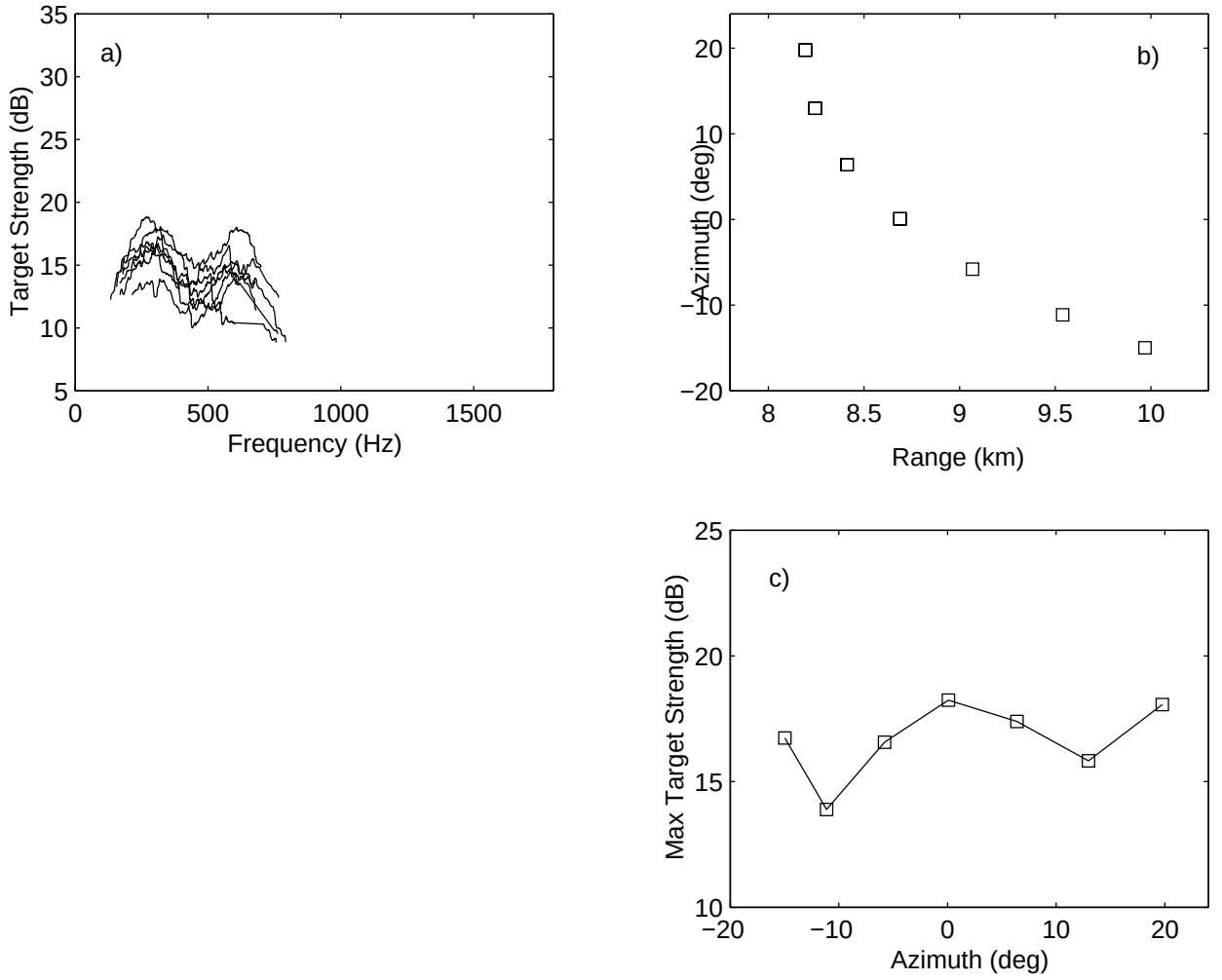


**Figure 18: Comparison of multiple observations of clutter from mud volcano a) target strength data, b) the dependence on range and azimuth from source/receiver to the mud volcano, c) correlation between maximum target strength and azimuth for the gas plume (x) and wreck (o).**

*Estimate of bubble size distributions*

Estimating the bubble size distribution from the sediment and the gas plume in the water column are crucial for understanding and future modeling of the clutter characteristics.

*Estimate of bubble size distribution in the sediment*

One of the potential mechanisms for the observed clutter (Figure 8) is scattering from bubbles close to the buried mud volcano vent. If bubbles are the dominant mechanism, their size distribution can be estimated by fitting the observed target strength with a model. The details of the inversion procedure are described in (Holland et al., in review). The estimated bubble size distribution is shown in Figure 19.

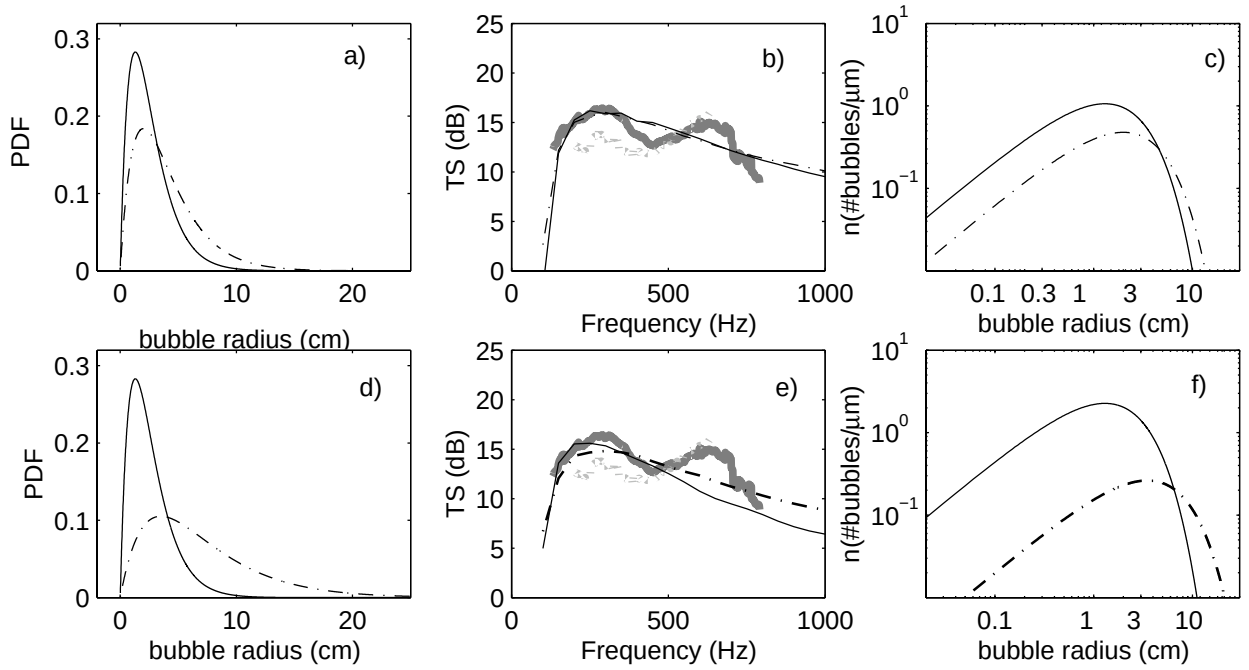


**Figure 19: Relationship between sediment bubble size distribution and target strength assuming sediment shear modulus of 1e6 Pa (black solid) and 2e7Pa (chain dash) a) modeled bubble size PDF, γ=5, b) modeled target strength and measurements at the buried mud volcano site (grey solid line) and gas plume site (grey dotted line), c) modeled bubble number density, c-d same as a-c except for spherical bubbles, γ=1.**

*Estimate of bubble size distribution in the plume*

By coupling a bubble evolution theory (how the bubbles evolve as they rise in the water column) to an acoustic scattering theory, a model for scattering from a bubble plume originating in the sediment can be predicted. The details of this model and how it was used in an inverse sense to predict the bubble size distribution is described in (Holland et al., in review). The resulting bubble size distribution is shown in Figure 20 and the analysis indicates that the clutter above about 650 Hz is due to scattering from bubbles in the water column. Below that frequency the scattering appears to be controlled by sediment-entrained bubbles.

*Summary of Malta Plateau analyses*

An important clutter mechanism in the Malta Plateau appears to be sediment-borne gas and gas ebullition in the water column. The gas frequently appears to be associated with mud volcanoes, i.e., conical structures whose peak may be completely below, near or even slightly above the surrounding seabed.

At the gas venting site, multiple reverberation observations made over time scales of an hour indicate that the gas venting is continuous (though variable) rather than pulsing or episodic. Observations over a decade suggest that there is a significant steady-state ebullition at that site.

Target strengths of 15-30 dB were observed, with a frequency dependence that was similar to that of a nearby wreck. There are three pieces of evidence that the target strength from 250-650 Hz is controlled by a different mechanism than from 650-1860 Hz. The latter frequency range is believed to be controlled by scattering from bubbles in the water column. The lower frequencies are believed to be controlled by scattering from sediment entrained bubbles. The first piece of evidence is that one of the pings with strong TS temporal variability above 650 Hz (interpreted as bubble plume variability) showed little temporal variability below 650 Hz. The second piece of evidence is the similarity between the frequency dependence of the 250-650 Hz target strength at the gas venting site and the buried mud volcano site. The third piece of evidence is that the bubble size distribution shows a clear null about 4-5 mm (corresponding to a resonance frequency of about 650 Hz), which may indicate two distinct bubble populations controlled by different formation, growth and decay mechanisms.

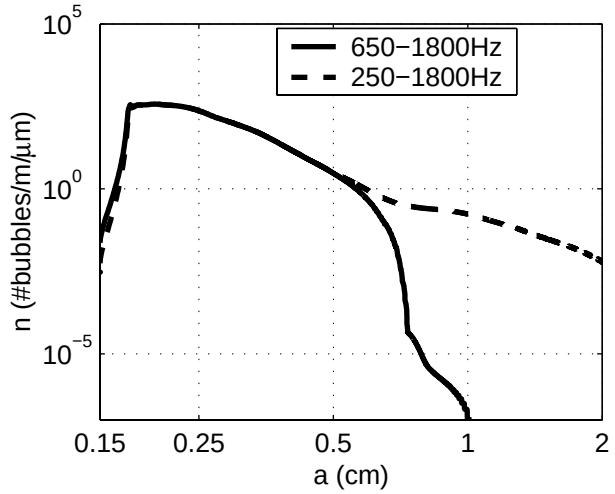


**Figure 20: The bubble size distribution for the entire water column. The two results shown correspond to the two different frequency ranges used in the inversion.**

Clutter at the buried mud volcanoes has a frequency dependence that is distinct from that of the wreck or the gas plume inasmuch as there is no measurable response above approximately 700 Hz. The clutter mechanism at this site is believed to be due to scattering from gas bubbles in the sediment. The gas bubbles appear to be entrained at a layer horizon approximately 3 meters below the water-sediment interface. In the vicinity of the mud volcano (but not near the vent) the estimated bubble size distribution has upper bound of approximately 0.3 cm. At the buried mud volcano (if bubble scattering is responsible for the clutter at this site), the bubble mean radius is an order of magnitude larger, approximately 3 cm.

The evidence for gas as the cause of the clutter consists of 1) co-located geophysical measurements that show gas ebullition and mud volcanoes (which are associated with gas emission) and 2) co-located acoustic reflection measurements that indicate gas-bearing sediments evidenced by rapid changes in reflectivity near the mud volcanoes (see Holland et al., in review). The potential physical mechanisms include scattering from the mud volcano structures (of order 10 m diameter), scattering from the gassy sediment (of order 50 m diameter) surrounding the

mud volcanoes and/or scattering from the gas released into the water column. The current hypothesis favors the latter two as the dominant mechanisms.

***Clutter Mechanisms Summary***

Sonar clutter can arise from a variety of features within the ocean environment. However, the potential environmental features are limited by two criteria: scale and impedance contrast. For ASW considerations, the scale of the features must be similar to the scale target, i.e., $O(10^1\text{-}10^2)$ m. Features much larger in extent may often be eliminated as potential targets because of differences in time spread (apparent spatial extent). The impedance contrast criteria is that only oceanic features with a large impedance (product of sound speed and density) difference to the surrounding host material should be considered as potential clutter feature. This is simply due to the fact that scattering from an object small impedance contrast (e.g., a sand lens imbedded in a silty-clay host, or internal waves) leads to small or undetectable response in the observed reverberation.

In practice, large impedance contrasts in the ocean are caused by the presence of gas (e.g., gas bubbles, gas in swim bladders, dissolved gas in sediment interstices), consolidated sediments (rocks) in contact with unconsolidated sediments (e.g., mud, silt, sand) and anthropogenic material. In the following, we consider potential scattering mechanisms from the sea surface, the ocean volume, the seabed and anthropogenic material.

*Sea Surface*

While the sea surface may generally lead to diffuse reverberation, it can potentially be a source of clutter for high-resolution sonar systems (e.g., Fialkowski et al, 2004) where the observed reverberation has been observed to exhibit non-Rayleigh statistics. The specific mechanism appears to be subsurface bubble plumes caused by wind-driven breaking waves.

*Ocean Volume*

Within the ocean volume itself, biologics are one potential clutter mechanism. Recent measurements have indicated that large fish schools can give rise to large sonar returns (Ratilal, et al., in review). It is not yet clear, whether such returns, which may have large time spreads, due to the spatial extent of the fish school would be classified as a potential target contact.

Another potential mechanism is gassy plumes originating from seabed. This mechanism was discussed in some detail in the preceding section.

*Seabed*

Seabed clutter mechanisms can be sub-divided into two categories, clutter events from the surface of the seabed and clutter events originating from buried or sub-seafloor features.

*Surficial features*

Surficial seabed features can be further subdivided into two categories, large-scale bathymetric features and small-scale bathymetric features. The division between the two scales is somewhat arbitrary, but is intended to divide those features which might be obvious on a bathymetric map with those of a scale that would not show up on a map. For example, shallow water ridges (see Makris, 1993 for a deep water example), escarpments, canyons could be on a bathymetric map (though arguably the mechanisms that cause the clutter, e.g., rock outcrops and facets, would be of a smaller scale and generally not on the map). Small-scale features (e.g., mud volcanoes) are unlikely to be represented on a map even produced with data from modern high-resolution multibeam sonar. In general, sand dunes/waves seem unlikely to produce clutter since the impedance contrast and the local slopes are small.

*Sub-bottom features*

A variety of geologic features could potentially lead to clutter including buried river channels, buried carbonate reefs (Max, 1996) or gassy sediments, especially those linked with small-scale structures like mud volcanoes. In addition, almost all of the surficial features that lead to clutter can also exist in the buried state. Not all forms of gassy sediments are expected to lead to clutter. For example, gas trapped below a layer of large extent might yield a large scattered return, but may have an associated time spread much larger than a potential target.

*Anthropogenic Features*

In some regions, off-shore oil exploration/production platforms exist, but these are easily mapped and probably would not be considered as potential false targets. Anthropogenic material frequently is associated with the seabed and may be at the surface of the seabed or buried. Examples would include, ship wrecks, well-heads, pipelines. Some of these features may be mapped, many are not.

**Base Program Task 2 – Evaluation Report on Diffuse Reverberation and Clutter Modeling**

The following section of this report summarizes a variety of reverberation models currently available including two Navy standard performance predictions models (ASPM and CASS), the high-frequency time series simulator (SST) and the more recent research of Chris Harrison (SACLANTCEN) and Kevin LePage (NRL-DC). Rather than attempt to summarize each of these approaches in this introduction, each of these approaches is described separately with a summary provided at the end of the section of the report.

***ASPM (Acoustic System Performance Model)*[2]**

The ASPM model is the first of two OAML approved models that will be discussed in this report. ASPM is a model designed for the prediction of detection performance of low frequency

[2] Text and information describing the ASPM model has been drawn from the OAML documentation for ASPM (references at end of this report).

active acoustic systems, operating with monostatic or bistatic configurations, in range-varying ocean environments. The core propagation loss model with ASPM is ASTRAL, which is also an OAML approved model. ASPM satisfies a number of system-level modeling requirements (Levin, SAIC-99/1008, 1999).

- Requirement 3.1-1: Model performance of active sonar systems below 4 KHz.
- Requirement 3.1-2: Model bistatic source/receiver geometries.
- Requirement 3.1-3: Model CW and FM signals.
- Requirement 3.1-4: Address effects of range and bearing dependent environments.
- Requirement 3.1-5: Provide reliable performance estimates in undersea environments in which the water depth is at least twelve times the wavelength of the lowest frequency of interest.
- Requirement 3.1-6: Use Navy standard models for propagation, bottom loss and surface loss.
- Requirement 3.1-7: Provide interfaces to Navy standard environmental databases.
- Requirement 3.1-8: Provide reverberation density estimates in a reasonable amount of time (1-10 minutes) on a Navy standard desktop computer.

As noted in the Software Design Document (Levin, SAIC-00/1032, 2000), the ASTRAL propagation loss model was selected to satisfy requirements 3.1-1, 3.1-4, 3.1-6 and 3.1-8. The ASTRAL propagation loss model has been approved up to 5 KHz, although several of the Navy standard environmental databases used by ASTRAL (and ASPM) have a more limited frequency range. The LFBL (Low Frequency Bottom Loss) database is currently approved for use from 50 Hz to 1 KHz with the HFBL (High Frequency Bottom Loss) database approved for use from 1.5 KHz to 5 KHz. The frequency gap between 1 and 1.5 KHz is handled using a “mixture” of the two databases (White, OAML-STD-23A, 2000). The ASTRAL propagation loss model is capable of modeling range dependent environments with bearing angle dependence treated using multiple radials originating at the source and receiver locations. The ASTRAL propagation loss model accepts the Navy standard databases for the prediction of low frequency bottom loss (LFBL) through its use of the LFBLTAB algorithm (Neumann, 1998) and at higher frequencies through the use of the HFBL bottom loss curves. The ASTRAL model uses the Navy standard model SRFLOS for the prediction of surface loss.

The final requirement that the use of ASTRAL satisfies in ASPM is 3.1-8, which relates to computational speed, but that requirement was achieved by making a compromise in the calculation of the reverberation by ASPM (Levin, SAIC-00/1032, 200). The arrival structure predicted by ASTRAL is not used throughout ASPM in the reverberation calculation. At each range-depth point for the reverberation calculation, the arrivals are combined to produce a single value for travel time, transmission loss, launch angle, angle at the reverberation point, etc. The first result of this approximation is that the effects of the source and receiver beam patterns are applied to the predicted arrivals from ASTRAL prior to the summation. Second, the time spread resulting from the multiple set of paths connecting the source to the range-depth point and the

paths connecting the receiver to the range-depth point is not included in the ASPM calculations for reverberation.

A presentation by Tony Eller (SAIC) at the OAML-SRB (Oceanographic and Atmospheric Master Library – Software Review Board) meeting in October 2003, listed the following as assumptions or perhaps more accurately approximations that make it possible for ASPM to produce these results on the current computing hardware.

- ASTRAL selected as propagation engine
- Do not save individual arrivals
- Assign single time for each range step in reverberation
- Factorable vertical/horizontal beam pattern
- Factorable bottom and surface scattering kernels
- Vertical beam patterns (source, receiver, scattering) applied in TL
- No extra convolution for time spread on two legs of path

Tony Eller continued with a list of pros and cons resulting from these assumptions.

- Primary Limitations
    - Accuracy
    - Resolution
    - Some detail not addressed
- Benefits
    - Computation time
    - Computer size, storage
    - Modularity allows rapid re-computation
- Mitigating Aspects
    - Environmental data uncertainties
    - Broad trends needed more than details for specific case

It was noted by Tony Eller in his presentation that any of these assumptions could be removed but at the cost of either increased computational time or a reduction in the physical area covered by the prediction.

The types of output generated by ASPM include both A-scan and B-scan displays of various quantities including reverberation (can be displayed by reverberation type), signal excess, etc. Figure 21 shows a graphic from Tony Eller's presentation showing signal excess for a

monostatic sonar. The capability of ASPM to provide predictions over a large geographic area for system with large coverage areas[3] is one of its key strength.

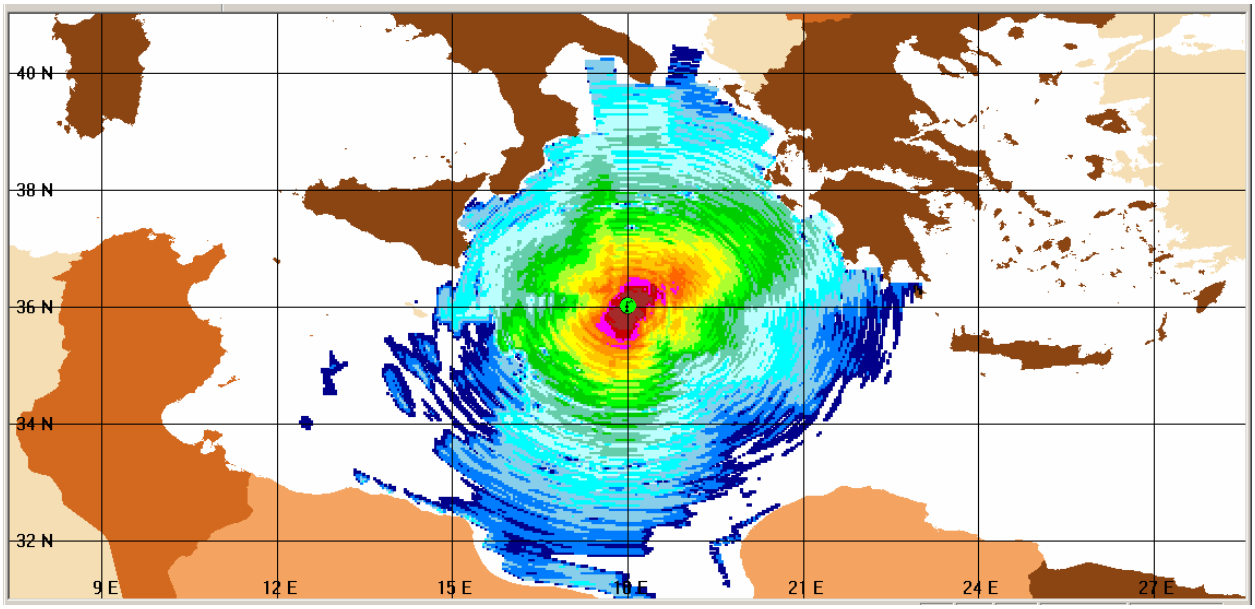


**Figure 21: Sample B-scan ASPM output showing signal excess for a monostatic sonar with a FM sweep source signal.**

ASPM can output a B-scan plot showing the total reverberation (referred to as combined reverberation) and component reverberation. The three components that contribute to the total reverberation in ASPM are sea-surface reverberation, volume reverberation, and ocean bottom reverberation. Seamount reverberation is combined with ocean bottom reverberation and presented as a single value in the reverberation output display and files. An example of the combined reverberation (all components) for the same sonar and location as shown in Figure 21 is provided in Figure 22.

ASPM is also capable of providing performance prediction for bistatic and multistatic geometries. The effects of range-dependent bathymetry and bottom properties are included in these calculations. A current limitation present in ASPM for calculating reverberation and bistatic and multistatic geometries is that the scattering kernels currently used for bottom and surface scattering do not include a dependence on the bistatic angle. This is a limitation caused the lack of a Navy standard model for ocean bottom scattering that includes the dependence on the bistatic angle. The current Navy standard bottom scattering kernel is the Lambert's Law.

$$S_B = 10\log\mu + 10\log(\sin\theta_{in}\sin\theta_{out})$$

The current Navy standard bottom scatter database for the frequency range of interest (between roughly 50 Hz and 5 KHz) uses a single value of $\mu = -27dB$, the Mackenzie coefficient, for the

[3] The area coverage of positive signal excess in Figure 21 is 15,776 square miles.

entire world (Mackenzie, 1961). It is clear that this bottom scatter kernel has no dependence on a bistatic angle. A brief explanation of the derivation of this expression is provided by Chris Harrison (Harrison, SR-356, pp. 46-47). The work of many researchers has shown that this expression for bottom scattering strength is of the wrong form for small grazing angles for ocean sediments with a sound speed ratio close to or less than one (Holland, 1996). The effect of scattering from the sub-bottom volume of the sediment and from sub-bottom scattering horizons was noted in the results of the CST program and has been included in the modeling work by many researchers over the past 10 years (Mourad, 1993; Yamamoto, 1996; Holland, 1998).

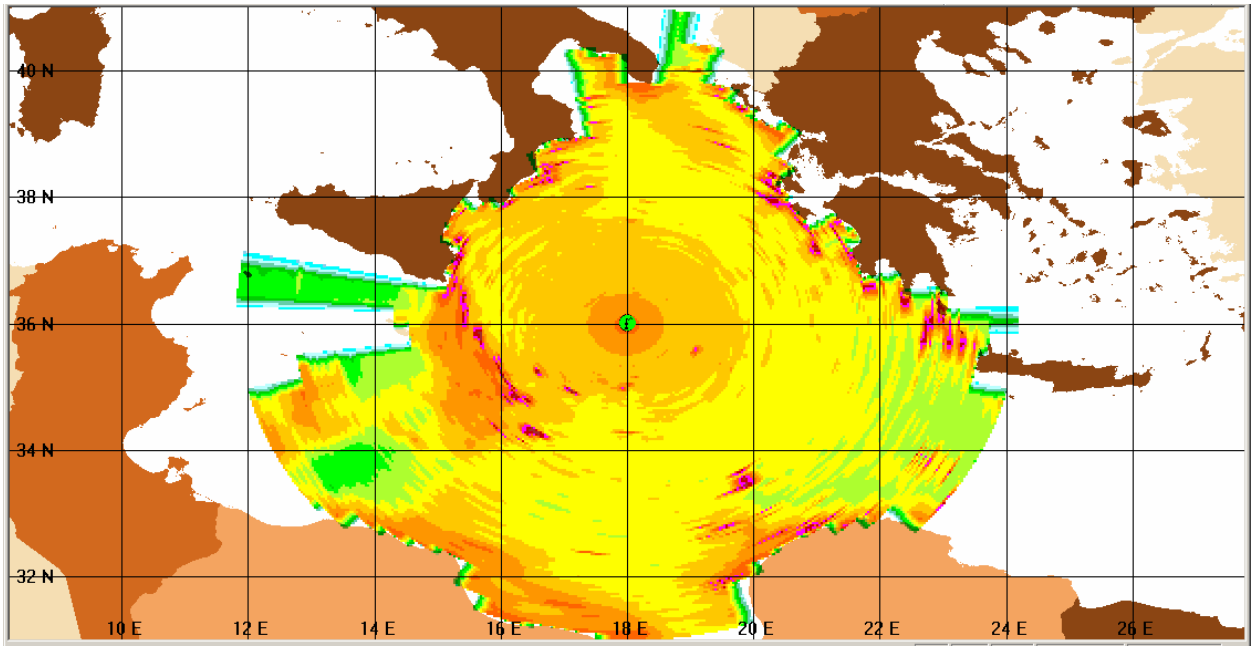


**Figure 22: Sample B-scan ASPM output showing the combined reverberation for a monostatic sonar.**

It should be noted that the Semi-Empirical Surface Scattering Strength (SESSS) algorithm version 1.0 was accepted as an OAML approved standard in April 2003 and the O-N-E algorithm was removed. The SESSS algorithm is the first broadband bistatic surface scattering strength (SSS) model for ASW application ($\leq 5000\text{Hz}$) (Gauss, 2000). The latest information provided by Roger Gauss (NRL-DC) is that the SESSS algorithm can be readily implemented into larger scale codes, such as the Active System Performance Model (ASPM) or the Comprehensive Active System Simulation (CASS) model within OAML.[4] It appears likely that, if funding is available, that the SESSS algorithm will be implemented in a future release of ASPM as the SESSS algorithm has replaced the O-N-E algorithm as the Navy standard surface scattering

[4] This comment was presented in a summary of the SESSS algorithm by Roger Gauss and Joseph M. Fialkowski submitted for survey paper edited by Peter Neumann on OAML standard environmental models and databases.

strength algorithm at ASW frequencies. An example of a signal excess prediction for a monostatic sonar with an adjunct array is shown in Figure 23.

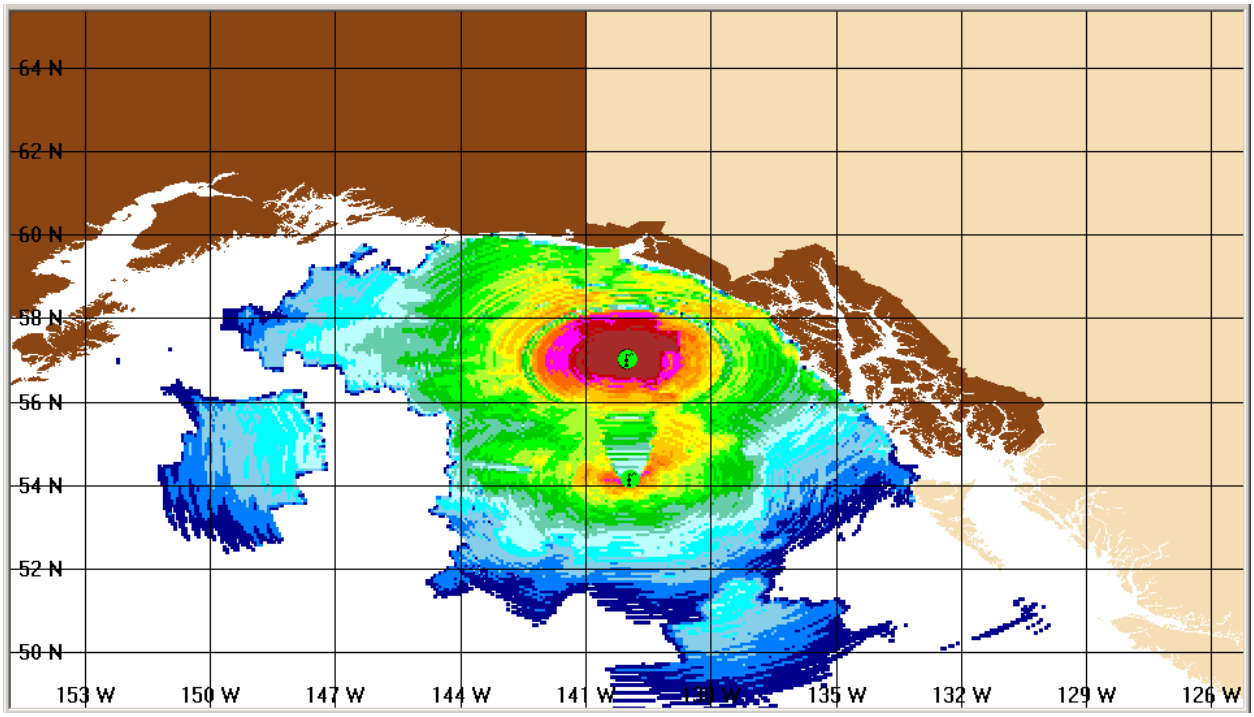


**Figure 23: Sample B-scan ASPM output showing the signal excess for a monostatic sonar with an adjunct array.**

The signal excess plot shown in Figure 23 is shown in Figure 24 for just the signal excess from the bistatic configuration. The figures shown in this section illustrate the capabilities of ASPM to perform performance prediction calculation for any location[5] in the world's oceans using the Navy standard databases. Within the non-configuration managed portion of ASPM, interfaces to the Navy standard databases including GDEM or provinced GDEM, DBDBV, and LFBL or HFBL. GDEM provides sound speed profiles as a function of latitude, longitude and season. DBDBV provides bathymetry at a variable resolution. LFBL provides geoacoustic parameters for the calculation of bottom loss at frequencies of 1 KHz and below. HFBL provides bottom loss for frequencies from 1.5 to 4.0 KHz in terms of nine different bottom loss curves.

The capability of ASPM to provide performance predictions for large geographic areas using Navy standard databases makes it a valuable tool for ASW mission planning. The Air ASW Tactical Decision Aid (TDA) ASPECT (Active System Performance Estimation Computer Tool) uses ASPM as its performance prediction engine. ASPM has provided on-board support for nearly all CST (Critical Sea Test), LFA (Low Frequency Active), ADI, LLFA (Littoral Low

[5] The geographic coverage of many Navy standard databases is not completely worldwide. As one example, the LFBL database used for calculating bottom loss at frequencies of 1 KHz and below does not include data for any location south of 49° S.

Frequency Active) and Magellan sea tests. ASPM has been incorporated in ASAPS (LFAPPS) and SPPFS and implemented into advance search planning models GRASP and MUSICAL.

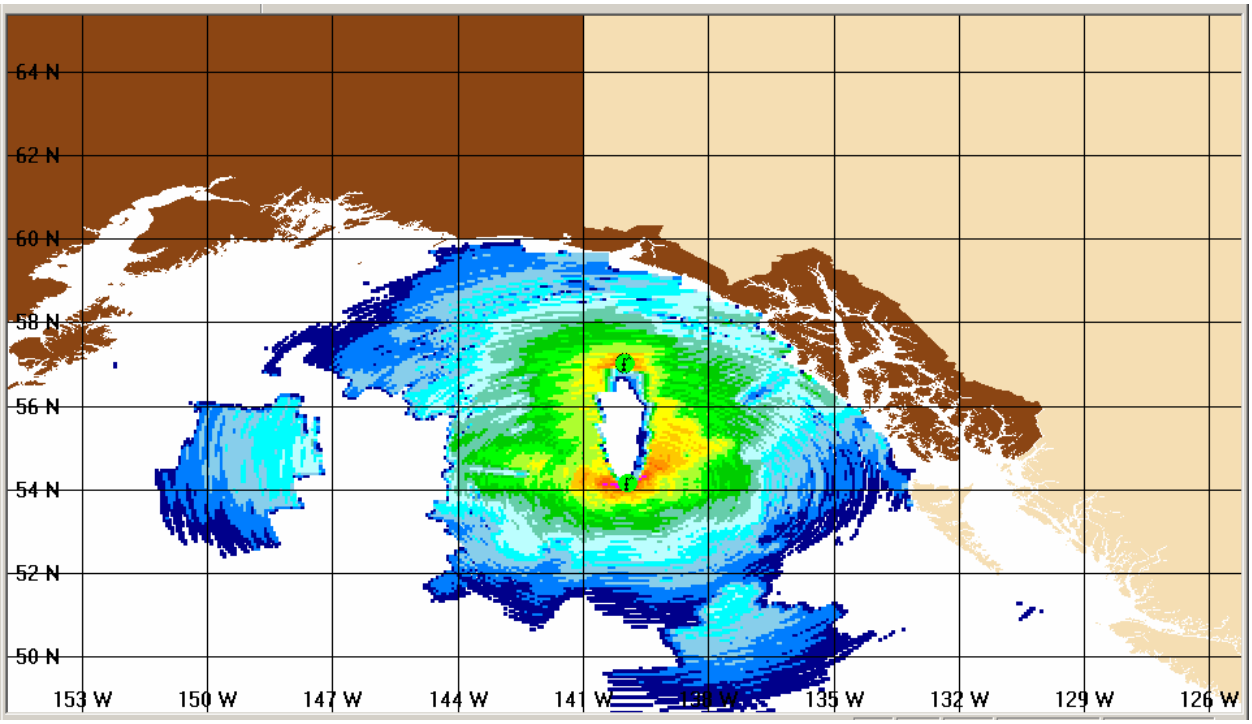


**Figure 24: Sample B-scan ASPM output showing the signal excess for just the bistatic configuration of the source and receiver.**

ASPM is a capable model for ASW mission planning but has some characteristics that make it an unsuitable choice for possible use as a broadband simulator for modeling discrete clutter and diffuse reverberation. A primary limitation of ASPM is that the modeling is done at the sonar equation level computing an output received level, reverberation level or signal excess for example. This choice makes ASPM considerably faster compared to most approaches that provide broadband time series simulations. In addition, the use of ASTRAL as the propagation loss model and more importantly the approximation of combining the many arrivals into a single arrival at each range-depth point, while necessary for the computational time constraints placed on ASPM, does not provide the level of accuracy required for accurate, broadband time series simulation. There is currently no provision for clutter modeling within ASPM.

The use of ASPM as a starting point for the broadband time series simulation of discrete clutter and diffuse reverberation, proposed under this Phase I STTR, would require the replacement of the propagation loss model, the scattering kernels for the ocean bottom, and the change from a sonar equation based computation to a time series based simulation to name just a few of the challenges. The strengths of ASPM in its application to ASW mission planning are its primary weaknesses when considered as a starting point for the proposed broadband time series simulation.

***CASS (Comprehensive Acoustic System Simulation)***

The CASS model[6] is the second of two OAML approved model that will be discussed in this report. Like the ASPM model, CASS is a Navy standard sonar performance prediction system that uses Navy standard environmental models and databases and Navy standard propagation loss models. The core propagation loss model within CASS is the Gaussian Ray Bundle (GRAB) model which is an eigenray model (Keenan, 2000) that is also used in the Sonar Simulation Toolset (SST) which will be the next model covered in this report.

The GRAB propagation loss model is an eigenray model capable of handling range-dependent environments. The environment is specified in independent, two-dimensional range-dependent surface, bottom and ocean grids. The range-dependent environment can include the specification of sound speed, temperature and salinity for the ocean grid. The bottom grid allows for specification of both bathymetry and bottom properties. GRAB includes the LFBLTAB routines for using the Navy standard LFBL database for the geoacoustic properties of the ocean bottom. For bottom scattering strength, CASS can use Lambert's Law with a Mackenzie coefficient of $\mu = -27dB$. At higher frequencies, there is also a mid-frequency bottom scattering kernel and the APL/UW bottom scattering strength curves for 10 KHz to 100 KHz are also implemented.

A key difference between CASS and ASPM is the details of their reverberation calculations. As noted in the previous section, ASPM computes reverberation from range-depth points discarding the time spread information provided by ASTRAL in the form of the arrival structure. CASS computes reverberation in the time domain using all the information provided by GRAB in the form of eigenrays that connect the source location to the scattering cell and the scattering cell to the receiver location. This does not mean that CASS computes a time series but that it computes all the possible combinations of eigenrays from the source location to the scattering cell and then from the scattering cell to the receiver location. These summed travel times are then assigned to the sampled time bins corresponding to the receiver signal processing being simulated. As noted in the IEEE Oceans 2000 article by Ruth Keenan, "CASS computes reverberation in the time domain by accounting for the leading and trailing scattering cell reverberation times for all possible combinations of eigenrays." This allows for such as effects as the transmitted pulse duration being longer than the sampled time bin length to be treated. Figure 25 shows how the ensonified area from a single combination of eigenrays, bounded by TIMMIN and TIMMAX, is divided between two time bins which are half the transmitted pulse duration, PLSLNG. The result is that CASS operates in the time domain unlike ASPM which operates in the range domain.

[6] CASS is often referred to as CASS/GRAB which links the CASS (Comprehensive Acoustic System Simulation) package with the GRAB (Gaussian Ray Bundle) propagation loss model. It is more correct to speak of GRAB being a component model used by CASS.

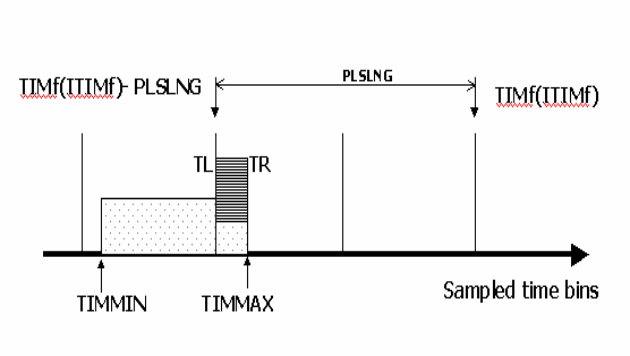


**Figure 25: CASS reverberation time binning (Keenan, 2000).**

Like ASPM, CASS uses the sonar equation for its calculations of reverberation level generating predictions in terms of a received level and not a time series. The computation of signal excess requires that the computed reverberation be compared with the computed signal from the target. Ruth Keenan describes this procedure in her article for IEEE Oceans 2000 this way, "CASS computes signal excess at each range step by mapping the signal into the time domain and picking the peak signal to noise/reverberation value. This approach implies that the signal used for the signal excess computation is not necessarily equal to the pressure level for the same range which represents the pressure integrated over all time." This process is illustrated in Figure 26 which shows how the peak reverberation level in each time bin is picked and then interpolated to the same time bin values as the signal level at which point the signal excess is calculated.

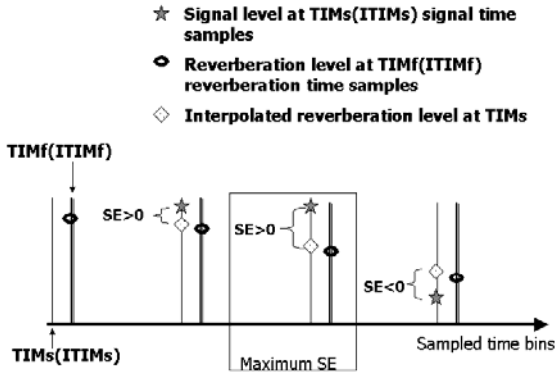


**Figure 26: CASS signal excess range binning (Keenan, 2000).**

This detail shows how CASS treats the calculation of reverberation in a more rigorous manner than ASPM but at the end of the calculation still reduces the signal excess to a single value for each time (or equivalently range) bin. Even with these computational improvements over ASPM, CASS is an unlikely candidate for use as a starting point for the broadband time simulation proposed under this STTR. The lack of any clutter modeling capability within CASS and the treatment of the ocean bottom using a reflection loss (through the use of LFBLTAB for frequencies of 1 KHz and below) also make CASS a poor candidate.

### *SST (Sonar Simulation Toolset)*[7]

The Sonar Simulation Toolset (SST) is a simulation package written by APL/UW to produce simulated sound as "heard" by a user-specified sonar system in a user-specified oceanic environment. The output of SST is a broadband signal that is intended to be realistic enough to "fool" the sonar processor (or operator) into behaving as if the sonar were at sea. This type of output separates itself from both ASPM and CASS and makes it a more likely candidate for the STTR modeling being developed for both discrete clutter and diffuse reverberation.

The current release of SST is able to simulate broadband time series with the following components.[8]

- Passive Signal: Sum of copies of source's transmitted signal, delayed, scaled, variably stretched or compressed for arbitrary maneuvers (Doppler shifts), and optionally filtered to reproduce frequency dependence of the ocean and beams.
- Source's Transmitted Signal: Broadband or tonal components generated by SST, or external signals from files.
- Target Echo: Sum of copies of source signal scattered from target highlights, delayed, scaled, Doppler shifted by sonar and target motion and optionally filtered by 2-way propagation, beam patterns, and highlights.
- Reverberation: Scattering of active sonar's ping from surface, bottom, volume. Scattering Function Method: A statistical description of the reverberation, the scattering function, is computed by integration. Gaussian reverberation is generated by convolving with pulse spectrum and randomizing.
- Background Noise: SST-generated Gaussian noise with specified spectrum, or any external signal from files, may be added to the simulated sound.

SST is designed as a different product from both ASPM and CASS covered earlier in this report. As a model that produces synthetic time series simulations for active and passive sonars, it is a simulator and not a sonar performance prediction model. The manner in which SST generates its synthetic time series is shown in Figure 27. Of particular importance to this evaluation is the calculation of the eigenrays[9] (top left corner of Figure 27) and the boundary reflection and scattering from the boundaries and water column volume (top right corner of Figure 27). The details on SST's calculation of each of these elements of its simulation will be covered in the following paragraphs.

---

[7] Text and information describing the SST package has been drawn from the documentation, reports and presentations on SST (references at end of this report).

[8] The list of components that SST is capable of simulating was taken directly from a PowerPoint presentation provided by Robert P. Goddard of APL/UW (Goddard, January 2002).

[9] Eigenrays define the propagation time (delay), ray direction at both the source and receiver location and the amplitude (real and imaginary) as a function of frequency.

SST computes the eigenrays using one of three different models. The most basic of the three eigenray models is one that uses a constant sound speed in the water column with specular reflections at the water-air and the water-sediment interfaces. This approach has the distinct advantage of speed but includes a range-independent water depth as its only environmental input. The second eigenray model is the GSM Eigenray model that either reads eigenray files computed by the Generic Sonar Model (GSM) or runs GSM as a subprocess to compute the eigenrays. GSM is also restricted to range-independent environments but does treat the interaction with the interfaces and the water column with more rigor than the first eigenray model discussed. The third choice for computing eigenrays is to use the CASS Eigenray Model which either reads eigenray files computed by CASS or runs CASS as a subprocess to compute the eigenrays. The propagation model used by CASS for the eigenray computation is the GRAB model discussed previously in the section of this report on CASS. Unlike the other two eigenray solvers, GRAB allows range-dependent environments.[10]

The generation of broadband time series by SST brings it much closer to the envisioned product of this STTR. The current options for calculating the eigenrays are unsuitable for low frequency (less than 1 KHz) simulations due to the use of the GRAB model as the eigenray engine for range-dependent environments. The treatment of the ocean bottom within GRAB at low frequencies parallels ASTRAL through the use of the LFBL database and the LFBLTAB model (Neumann, 1998). The output of LFBLTAB does not include the time spreading generated by a layered sub-bottom. The prediction from LFBLTAB includes the reflection loss which is more accurately described as a total energy bottom loss as it includes all the energy from reflection at the water-sediment interface and energy refracted back into the water column due to the sound speed profile in the sediment. At the frequencies for which SST is normally utilized, the treatment of the ocean bottom as a reflecting interface with a reflection loss value and no time spread is certainly adequate. However, accurate simulation of time series at frequencies below 1 KHz requires a more robust treatment of the interaction of the acoustic energy with the ocean bottom.

The scattering kernels for the surface and bottom within SST are handled using a variety of models available to the user. For the sea surface, there are three models available including the APL Surface model which is a monostatic, high frequency model including the effects of sea surface roughness, surface facets and sub-surface resonant bubbles. The McDaniel Surface model extends the APL Surface model as a bistatic, high frequency model with similar physics (McDaniel, 1990). The third model is the Gilbert Surface model which is a bistatic, low to mid-frequency model including the effects of sea surface roughness, surface facets and treating the sub-surface bubble clouds as non-resonant with random sound speed perturbations (Gilbert, 1993).

[10] GRAB treats range-dependence as a set of N by 2-D environments where N represents the number of radials originating at a source and/or receiver. This is the same approach to range-dependence used by ASTRAL in its implementation in ASPM.

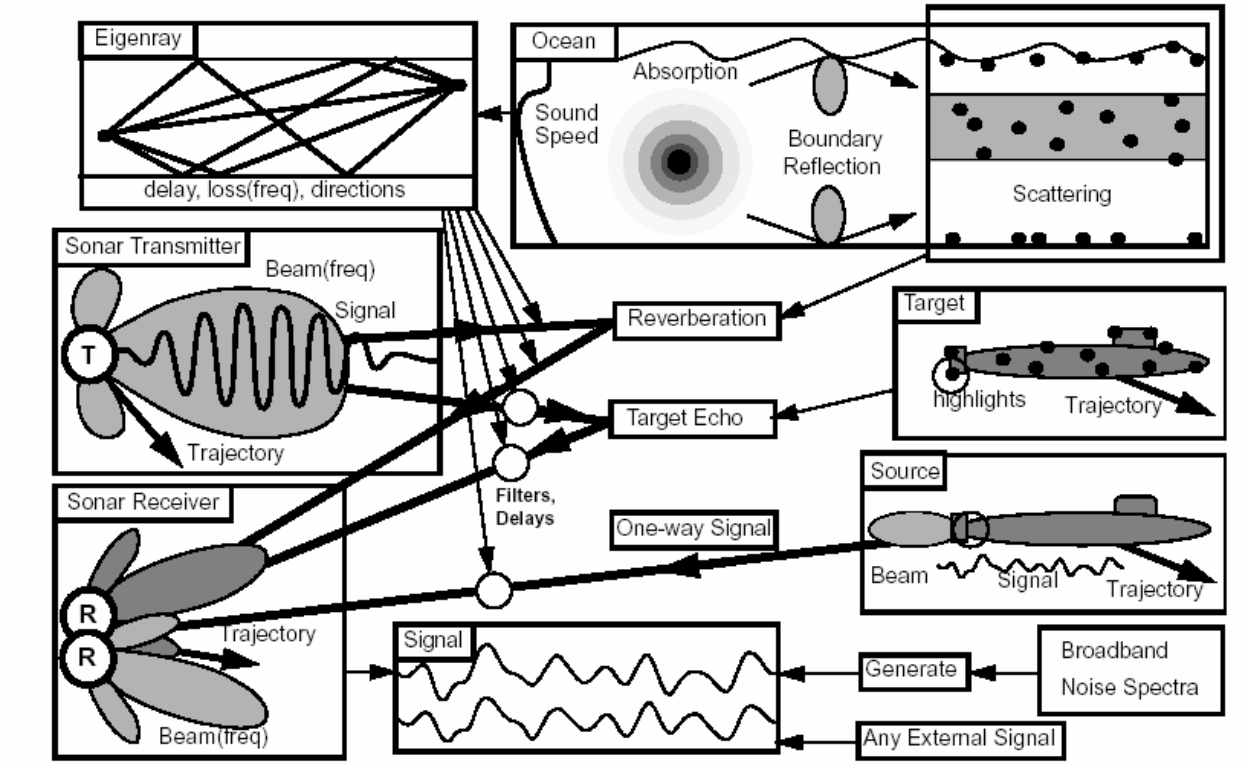


**Figure 27: SST Component Models.**

There are two ocean bottom models both of which are monostatic. The first is a functional representation of the scattering kernel, such as Lambert's Law, with a functional dependence on the incident and scattered grazing angles. This representation has no dependence on the bistatic angle so the bistatic scattering strength is currently taken as the dB average of the incident and scattered grazing angles. The second bottom scatter kernel available in SST is the APL Bottom which is a high frequency, monostatic modeling approach. Developed at APL/UW, this modeling approach uses a Rayleigh reflection coefficient for forward reflection loss and the Kirchhoff approximation, composite roughness, large-roughness correction and volume scattering (Jackson, 1986; Jackson, 1992; Williams, 1998).

Robert Goddard provided a list of potential future upgrades to SST in a draft August, 2003 journal article (no reference currently available). Of most interest to this STTR is the proposal to extend SST's capabilities down to lower frequencies. In the draft article, Goddard writes, "Farther reaching changes would extend SST's applicability down to lower frequencies. A bottom model with penetration to sub-bottom layers would be a good start. A more radical change would be to incorporate some form of Parabolic Equation (PE) or other wave-based propagation model."

Discussions with Robert Goddard in October 2003 on the topic of extending SST to lower frequencies (less than 1 KHz) revealed the scope of this task to be larger than anticipated. The integration of a new propagation loss model (PE or some other wave-based model) would likely have to be done by APL/UW as they hold the intellectual property rights to SST and are

responsible for maintaining the coding standards used within SST. The current practice of using eigenray information to produce the synthetic time series also has its short-comings when applied to environments with multiple sub-bottom layers. The number of eigenrays increases to an unmanageable number with just a few sediment layers due to the splitting of the eigenray at each sediment layer interface. The advantages to using SST as a starting point are that it is a mature and stable product that is designed to generate simulated time series realizations for both active and passive sonars.

***Reverberation Modeling Work by Chris Harrison***

Recent work at SACLANTCEN by Chris Harrison and collaborators has resulted in the development of a model-based multistatic performance prediction tool called SUPREMO as well as analytic formulae useful for quickly and accurately predicting diffuse reverberation levels for certain types of environments.

The SUPREMO tool is designed to predict reverberation, target return and noise for general environments, with a user specified level of accuracy (Baldacci et al., 2002). It is modular, with the transmission loss kernel interchangeable. The overarching SUPREMO tool, which is built in MATLAB and includes a GUI, requires the transmission loss model selected or incorporated by the user to return the incident intensity on the scatterers (bottom, target and free surface) as a function of grazing angle and time at a given spatial location. Currently this quantity is supplied by GAMARAY for range independent environments, and BELLHOP for range dependent environments. The SUPREMO shell creates input files for general multistatic propagation from sources to scatterers, and from the scatterers to the receivers, including vertical aperture effects. To increase efficiency, the beam-time space at the receiver is randomly populated at a user specified density, and then mapped to geographical space and triangulated into elementary scattering patches using Delauney triangulation. Reverberation predicted in beam-time space from the scattering patches is then convolved with the array response in angle and the matched filter response in time to predict reverberation as seen by a particular system for the specified environment. The density of the sampling in beam time space, and the degree of fidelity of the angle-time intensity predictions at the scatterers controls the overall fidelity of the resulting prediction.

The approach taken in SUPREMO could be extended to the prediction of reverberation time series and clutter with some modification. The return from each scattering patch would be the convolution of the angular decomposition of the incident field and scattered field at each scattering patch with some realization of scatterers on that patch, dependent again on incident and departing grazing angle and the bistatic angle. Ideally the returns from adjacent patches would be correlated. Discrete scatterers would be handled in the same way.

Recently Chris Harrison has derived complimentary analytic predictions of diffuse reverberation for bistatic scenarios in range dependent environments with either isovelocity or constant sound speed gradients (Harrison, 2003, 2002a,b,c; Prior, 2002). The power of this predictive capability cannot be overestimated. The reverberation predictions are very fast and agree closely with more laboriously obtained predictions. The existence of this rapid predictive capability for reverberation intensity raises the possibility of quickly estimating the second moment of

reverberation pressure for environments of interest and then generating consistent time series with higher moments that conform to advances in understanding of the time evolution of non-Rayleigh reverberation as obtained by Lyons, Abraham and others. This non-Rayleighness would be parameterized on such system parameters as center frequency, time-bandwidth product and horizontal beamwidth, and environmental parameters such as the correlation length scale of the scatterers and the number of important ensonifying multipath (also controlled by vertical aperture at the source and receiver.) The resulting tool would comprise a parametric predictive capability for clutter and diffuse reverberation time series based on the physics of propagation, ensonification and scattering derived by Harrison and the statistics of the distributions of reverberation time series as derived by Lyons, Abraham and others.

***Reverberation Modeling Work by Kevin LePage***

Modeling approaches developed by Kevin LePage at SACLANTCEN and NRL-DC (LePage, 2003; LePage et al., 2003; LePage, 2002a,b; Bouchage et al., 2002; LePage et al., 2000; LePage 1999) are appropriate for directly modeling reverberation time series in the low to mid frequency regime. LePage's work relies on the fact that normal mode methods are directly applicable for predicting time series in narrow bands[11] to efficiently predict reverberation from arbitrary distributions (realizations) of scatterers. The approach is most efficient for monostatic geometries and range independent environments, but has been extended to range dependent environments and bistatic geometries for reverberation intensity. Reverberation time series estimation for the more general environments and source/receiver geometries should be relatively straightforward although the correlation of neighboring bistatic reverberation patches would have to be addressed. More details and examples of this work are provided in the section of this report titled "Base Program Task 3 – NRL-DC Modeling Support."

***Requirements for Broadband Time Series Modeling from the EER and LAMP Programs***

In a meeting held on December 11th, 2003, the applicability of the proposed broadband time series simulation to the EER and LAMP programs was explored. The primary goals of the meeting were to brief the representatives of these programs on the plans and objectives of this Phase I STTR proposal and to solicit their program requirements. The attendees at the meeting were the following individuals (listed by name, telephone number and email address).

- John H. Joseph (301) 342-2121 john.joseph@navy.mil
- David Bromley (301) 342-2116 david.bromley@navy.mil
- David Fenton (301) 342-2050 david.fenton@navy.mil
- Dan Flynn (301) 342-2051 daniel.f.flynn@navy.mil
- Don Russo (301) 342-2048 donato.russo@navy.mil
- Greg Muncill (301) 706-4951 gmuncill@mindspring.com

[11] Approximately one tenth of the center frequency (LePage 2001).

- Kevin LePage (202) 404-4834 kevin.lepage@nrl.navy.mil
- Rick Fillhart (301) 342-2078 ricky.fillhart@navy.mil
- Peter Neumann (540) 552-5102 pneumann@plansys.com

*Prepared Material for Meeting:*

Discussion began with an overview of the Phase I STTR (topic N03-T011) currently underway by PSI (Peter Neumann and Greg Muncill), ARL/PSU (Charles Holland) and NRL-DC (Kevin LePage).

*Overview of Phase I STTR*

- STTR Topic N03-T011 – "Physics-based modeling of acoustic reverberation in the littoral environment"
- Phase I STTR proposal titled – "Advanced Physics-Based Modeling of Discrete Clutter and Diffuse Reverberation in the Littoral Environment"
- TPOC for the Phase I STTR is James McEachern (ONR Code 321SS)
- Period of performance is 1 July 2003 through 2 February 2004 for the Phase I STTR

*Key Goals of the STTR*

- Develop a simulation capability (broadband time series) that accurately predicts discrete clutter and diffuse reverberation
- Output time series for each sensor element
- Handles bistatic geometries
- Treats Doppler
- Handles range-dependent environments (bottom properties, sound speed profiles in the water column, bathymetry, …)
- Frequency range is up to 4-5 KHz and down to the lower limit for normal mode propagation modeling

*Application to Design (Build-Test-Build) of Coherent, Active Air ASW Source (AEER)*

- Can reduce the in-water testing costs by using simulation
- Able to simulate sensor performance with various signal processing algorithms
- Able to simulate target-like returns from discrete clutter in addition to mean reverberation level

*Design Issues for the Simulation to be Addressed*

- Programming language (Fortran, C, C++, Matlab, …)
- Hardware (PC, Linux, …)
- Run-time speed (not real-time but run-time is important design criteria)
- Integration of simulation with signal processing routines/hardware

*Potential Phase II Award*

- Letter of endorsement for proposed simulation package from the AEER program and the LAMP program would be quite helpful in securing Phase II award
- Letter of endorsement states the program's interest in evaluating the products of the Phase II award (simulation package) within their program objectives and requirements (active, coherent source design)

*Notes from Meeting:*

The following are notes taken by Peter Neumann, Kevin LePage and Greg Muncill at the meeting.

*Requirements for AEER program (NAWC)*

- Can accept simulation package in either Fortran or Matlab (appears that Matlab would be the easiest for integration into their work)
- Simulation must be able to include the frequency spread (widening of the Doppler ridge) due to the surface interaction/scattering
- Requires beam formed output instead of element level output (requires detailed information on element locations and beam forming algorithms)
- Must be able to simulate various waveforms (CW, HFM – bandwidth of signals up to 10% of center frequency of signal)
- OAML approval or a peer review validation and verification (V&V) would an essential requirement for their use of the proposed simulation package
- Simulation must be able to handle multiple pings with ping reverberation overlap (multiple pings at intervals shorter than the time for the reverberation to decay to the background ambient noise level)

*Requirements for LAMP program (ONR)*

- Simulation must be able to go down to 400 Hz

*Data Sources Available for Phase II Simulation Development*

- Rick Fillhart – AEER (approximately 850 Hz), IEER

- APL/JHU – MACE (approximately 450 Hz)
- UK – ALFEA (Airborne Low-Frequency Electro-Acoustic) (approximately 1.8 KHz)

*Action Items*

- Email Phase I STTR proposal to Rick Fillhart
- Schedule a brief (with ONR and NAWC) at the end of the Phase I
- Email summary of December 11th meeting to attendees, Jim McEachern (ONR) and Charles Holland (ARL/PSU)

**Base Program Task 3 – NRL-DC Modeling Support**

***Modeling of clutter in diffuse reverberation***

The reverberation model developed at NRL-DC has been exercised to evaluate clutter like characteristics of reverberation in a notional shallow water environment (LePage, 2004). Recent work by Abraham and Lyons (Abrahams et al., 2003) has shown that exponentially distributed scatterers yield K-distributed reverberation envelopes for saturated propagator phase in direct path ensonification scenarios. In their work the shape parameter $\nu$ of the K-distribution was found to be proportional to the number of ensonified scatterers. This number is controlled by the horizontal aperture of the source/receiver system, the vertical aperture for early times, the bandwidth for late times, and the representative scale on which the scatterers are distributed (correlation length scale.) Their results showed that the reverberation envelope became essentially Rayleigh for more than 40 independent scatterers ($\nu$=20.) To study how these results would change with the introduction of multipath, the NRL-DC reverberation time series model was exercised for both exponential and Gaussian distributed bottom scatterer realizations ensonified over the 5-750 Hz band, for both single path (single mode) ensonification and scattering (corresponding to mode 1 filtering on the source and receiver,) and the full multipath ensonification consistent with measurement of reverberation excited by a point source and measured on a single hydrophone.

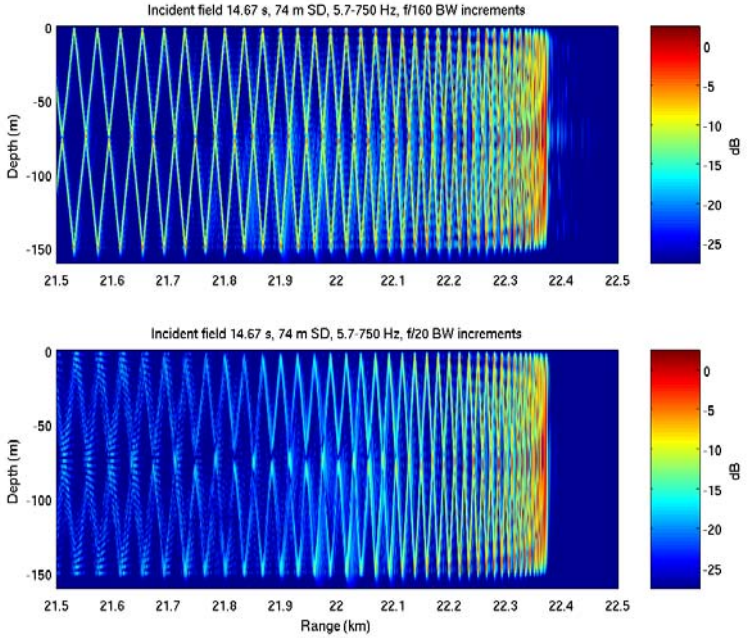


**Figure 28: Exact (top) and approximate incident time series in notional shallow water waveguide.**

The environment selected is an almost isovelocity winter profile in 150 m of water overlying a fast sandy sediment with a background sound speed of 1702 m/s, a density of 1.85 gm/cm$^3$ and attenuation of 0.173 dB/λ. The critical angle of this bottom is 26.3°. An example of the field in this waveguide at a time of 14.67 s after the shot for a source depth of 74 m is shown in the top panel of Figure 28. In the bottom panel is shown the narrowband approximation for the field utilized to obtain the results in this section (it is assumed that the approximation in the lower panel is sufficient to describe the incident and scattered field to and from the scatterers.) The expression for the incident pressure in a narrow band is

$$p\left(t,r,z\middle|\omega_o,z_s\right)\simeq\sum_{n=1}^{N}\left(1/\Delta\omega^2-i\frac{\partial^2 k_n}{\partial\omega^2}r\right)^{-1/2}\frac{\phi_n\left(z_s\right)\phi_n\left(z\right)}{\sqrt{k_n r}}\exp\left(-\left(t-\frac{\partial k_n}{\partial\omega}r\right)^2\Big/\left(2/\Delta\omega^2-i2\frac{\partial^2 k_n}{\partial\omega^2}r\right)\right)$$

where $\omega_o$ is the center frequency, $\Delta\omega$ is the corresponding bandwidth and all the properties of the normal modes and the frequency derivatives are evaluated at the center frequency. The consistent expression for the reverberation in a narrow band is

$$p_{rev}\left(t,z\middle|\omega_o,z_s\right)\simeq\sum_{m=1}^{N}\sum_{n=1}^{N}\int_0^\infty dr\frac{\sqrt{2\pi}\phi_n\left(z_s\right)\xi_n^-\left\langle\eta\left(r,\theta\right)\right\rangle_\theta\xi_m^+\phi_m\left(z\right)}{\sqrt{\left(1/\Delta\omega^2-i\frac{\partial^2\left(k_n+k_m\right)}{\partial\omega^2}r\right)k_n k_m}}\exp\left(-\frac{\left(t-\frac{\partial\left(k_n+k_m\right)}{\partial\omega}r\right)^2}{\left(2/\Delta\omega^2-i2\frac{\partial^2\left(k_n+k_m\right)}{\partial\omega^2}r\right)}\right)$$

In the work presented here $\xi_n^-$ is the product of the downgoing modal amplitude $\phi_n^-$ (derived from the mode shape function $\phi_n$ under the WKB approximation,) and the square root of the pressure equivalent of the separable scattering function $SS_{nm}$ obeying Lamberts law, i.e.

$$\xi_n^- = 10^{-27/40}\sqrt{\sin\left(a\cos\left(k_n/k_o\right)\right)}\phi_n^-,$$

and $\xi_n^+$ is it's upgoing analog

$$\xi_m^+ = 10^{-27/40}\sqrt{\sin\left(a\cos\left(k_m/k_o\right)\right)}\phi_m^+.$$

The roughness function $\eta(r,\theta)$ itself is a zero mean random variable with an isotropic correlation length scale which has been azimuthally averaged to obtain $\langle\eta(r,\theta)\rangle_\theta$. The length scale is chosen to be less than a wavelength in order to rule out undesired reductions in backscattering due to Bragg scattering effects, thereby forcing the resulting reverberation time series to mimic in angular content and amplitude reverberation from a surface whose scattering function obeys Lamberts law.

Narrowband approximations for the reverberation time series at various frequencies may be coherently summed as long as the same azimuthally averaged roughness realization is used. In this way broadband predictions of reverberation may be obtained using the narrowband approximation. Figure 29 shows the frequency content of 74 narrowband approximations for reverberation from the same roughness profile over the 17-750 Hz band. Since the narrowband approximation works best for bandwidths less then $\omega_o/10$, the interval between each narrowband approximation increases linearly with frequency. As opposed to fast Fourier synthesis, the frequency interval is not dictated by the desired length of the synthesized time series, and the frequency interval is not required to remain the same over the frequency band of interest.

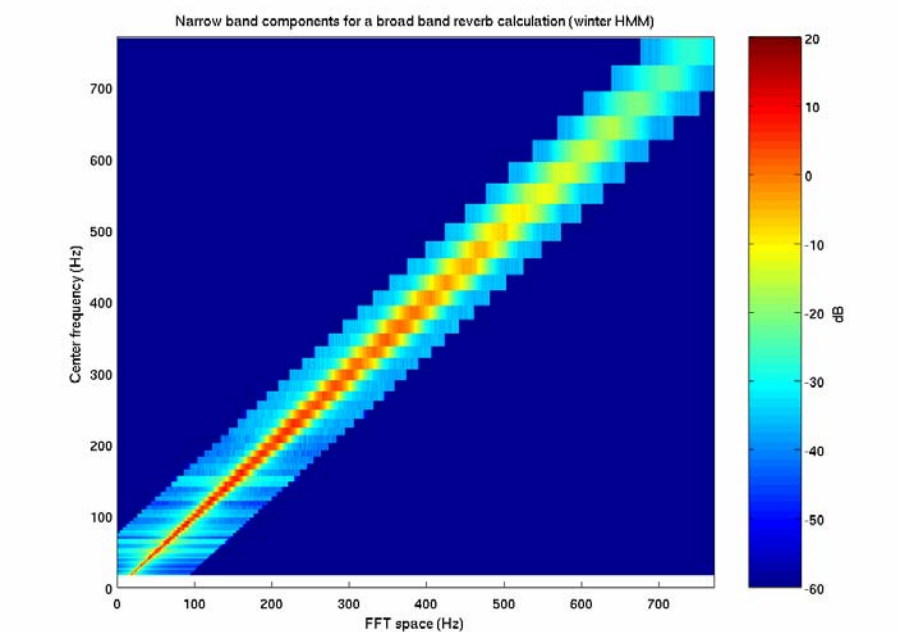


**Figure 29: Frequency content of superimposed narrowband approximations.**

We compare the statistics of broadband reverberation caused by two scatterer profiles. The first scatter profile is distributed Gaussian in amplitude and had a 1 m correlation length scale. The second realization is exponentially distributed in amplitude with the same correlation length scale. The azimuthal averages of the two realizations are shown in Figure 30.

In Figure 31 the resulting broadband reverberation time series for scattering from the roughness height distributions in Figure 30 are shown. It is possible to see that there are more high amplitude clutter-like outliers in the early time portion of the exponentially scattered time series (bottom panel) then there are in the reverberation from the Gaussian distributed scatterers (top panel.) In Figure 32 the sample pdfs (probability density functions) of the reverberation envelope for the exponentially distributed scatterer scenario are shown in the top panel. In the lower panel the K-distribution shape parameter ν is shown as a function of time after shot. It is seen that the reverberation is significantly non-Rayleigh ($\nu<20$) for the first 3-5 s after the shot, due to the small number of illuminated scatterers. However, for greater times the reverberation becomes essentially Rayleigh, due to the large number of resolved multipath and the consequentially larger number of illuminated independent scatterers on the bottom. For reference, the time evolution of the pdf and the K-distribution shape parameter for the Gaussian distributed roughness realization is shown in Figure 33, indicating Rayleigh reverberation characteristics for all but the earliest times.

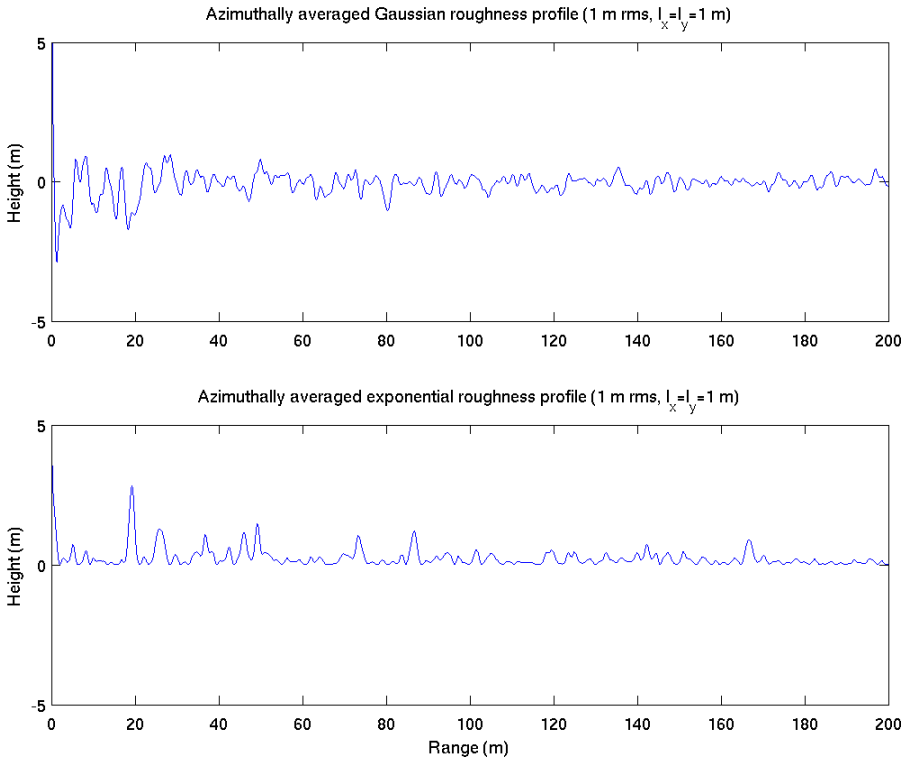


**Figure 30: Gaussian (top) and exponentially (bottom) distributed bottom roughness amplitudes used to estimate reverberation envelope.**

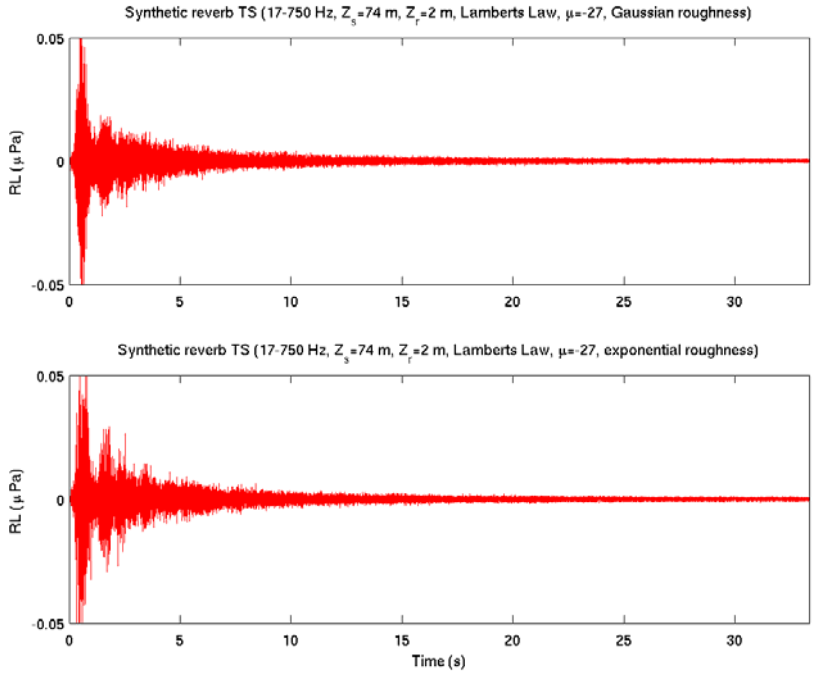


**Figure 31: Reverberation time series scattered by Gaussian (top) and exponentially (bottom) distributed bottom roughness amplitudes.**

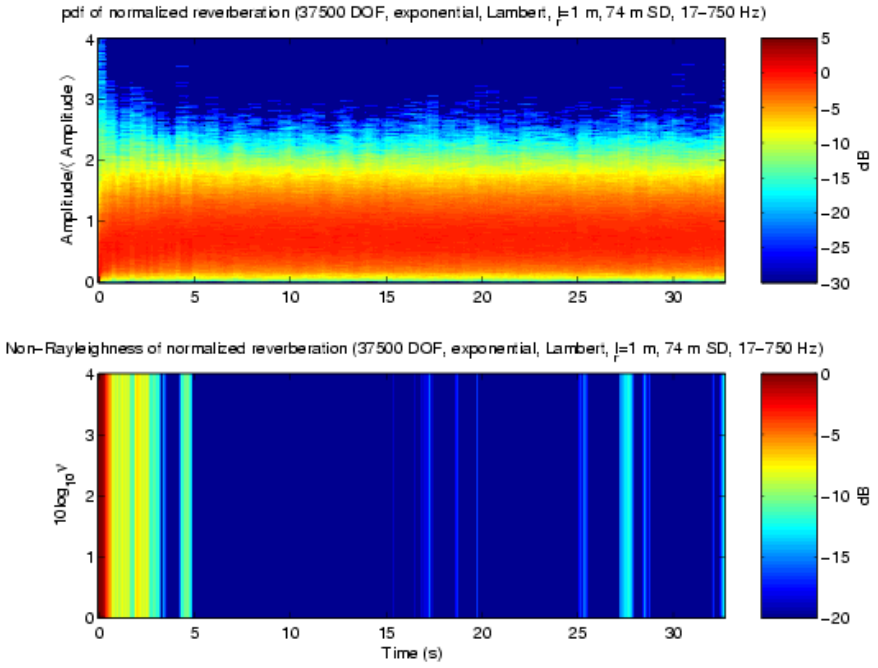


**Figure 32: Sample pdf (top) and 10 log10 of the K distribution shape parameter ν (bottom) of broadband reverberation from exponentially distributed scatterers.**

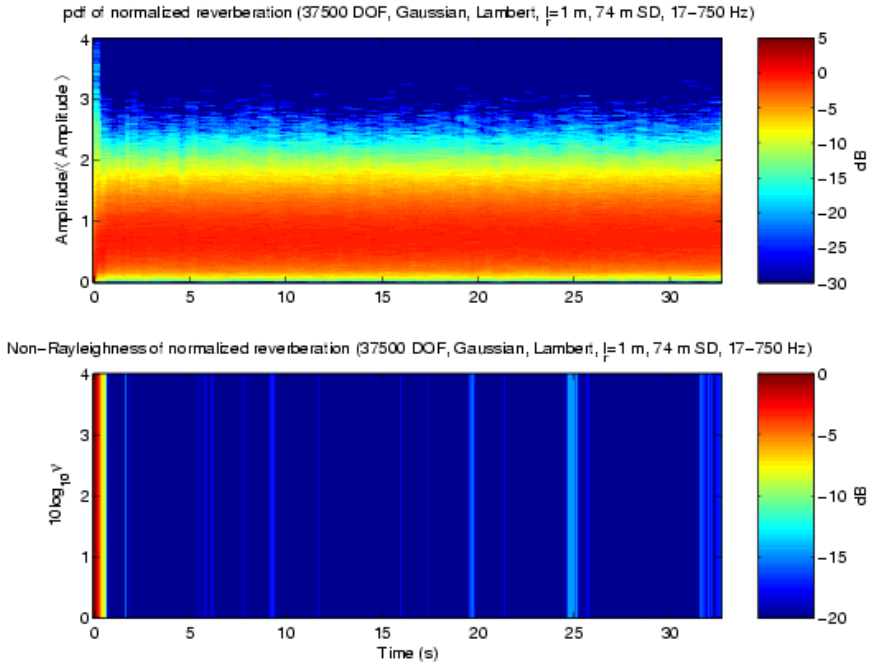


**Figure 33: Sample pdf (top) and 10 log10 of the K distribution shape parameter ν (bottom) of broadband reverberation from Gaussian distributed scatterers.**

***Modeling of clutter-like returns from discrete scatterers***

Preliminary studies into the modeling of clutter-like returns from discrete scatterers have also been conducted. This work builds upon the approaches developed at NRL-DC for modeling diffuse reverberation in range dependent environments using coupled mode theory. One-way propagation in range dependent environments is well approximated as (Ferla et al., 1993)

$$p^j\left(r,z\middle|\omega_o,z_s\right)\simeq\sum_{n=1}^{N^j}a_n^j\frac{H_o^1\left(k_n^jr\right)}{H_o^1\left(k_n^jr_{j-1}\right)}\phi_n^j\left(z\right)$$

where

$$a_n^1\doteq\frac{i}{4\rho\left(z_s\right)}\phi_n\left(z_s\right)H_0^1\left(k_n^1r_1\right)$$

and under the impedance matching condition

$$a_n^{j+1}=\int_0^\infty dz\sum_{m=1}^{M^j}a_m^j\frac{H_0^1\left(k_m^jr_j\right)}{H_0^1\left(k_m^1r_{j-1}\right)}\frac{\phi_m^j\left(z\right)\phi_n^{j+1}\left(z\right)}{\sqrt{\rho_j\left(z\right)\rho_{j+1}\left(z\right)c_j\left(z\right)/c_{j+1}\left(z\right)}}.$$

Under the single scattering and azimuthally symmetric approximation, the *backscattered* field at each range step is

$$p_{BS}^{j}\left(r,z\middle|\omega_o,z_s\right)\simeq\sum_{n=1}^{N^j}b_n^j\frac{H_0^2\left(k_n^j r\right)}{H_0^2\left(k_n^j r_j\right)}\phi_n^j\left(z\right),$$

where under continuity of pressure and horizontal velocity at each interface (Jensen et al., 1994)

$$b^j=-\left[R_4^j\right]^{-1}R_3^j a^j$$

or

$$b_m^j=T_{mn}^j a_n^j$$

where

$$R_{4\,nm}^j=\frac{1}{2}\left(\int_0^\infty dz\frac{\phi_m^{j+1}\left(z\right)\phi_n^j\left(z\right)}{\rho_{j+1}\left(z\right)}+\frac{k_m^{j+1}}{k_n^j}\int_0^\infty dz\frac{\phi_m^{j+1}\left(z\right)\phi_n^j\left(z\right)}{\rho_j\left(z\right)}\right)\frac{H_0^2\left(k_n^j r_{j+1}\right)}{H_0^2\left(k_n^j r_j\right)}$$

$$R_{3\,nm}^j=\frac{1}{2}\left(\int_0^\infty dz\frac{\phi_m^{j+1}\left(z\right)\phi_n^j\left(z\right)}{\rho_{j+1}\left(z\right)}-\frac{k_m^{j+1}}{k_n^j}\int_0^\infty dz\frac{\phi_m^{j+1}\left(z\right)\phi_n^j\left(z\right)}{\rho_j\left(z\right)}\right)\frac{H_0^1\left(k_n^j r_{j+1}\right)}{H_0^1\left(k_n^j r_j\right)}.$$

Using Green's theorem, the local backscattered pressure and velocity at the scatterer may be integrated over the scatterers horizontal trajectory in the [*x,y*] plane in order to determine the total scattered field. Assuming for simplicity range independent propagation along the horizontal *x* axis from the source to the scatterer, the phase of the incident field can be expanded to second order in the scatterer trajectory *X*(*y*) yielding the following approximation for the scattered field

$$p_{scat}\left(R_s,z_s,z_{scat},X\left(y\right),y\right)\simeq C_i\sum_{m=1}^{N}\sum_{n=1}^{N}\frac{\phi_n\left(z_s\right)T_{nm}\phi_m\left(z_{scat}\right)}{\sqrt{k_n}}\exp\left(ik_n\left(R_s+\frac{\partial X\left(y\right)}{\partial y}y+\frac{1}{2}\left(\frac{\partial^2 X\left(y\right)}{\partial y^2}+\frac{1}{R_s}\right)y^2\right)\right)$$

where

$$C_i=\sqrt{2\pi}e^{i\pi/4}/\rho\left(z_s\right)\sqrt{R_r}$$

while the phase from the scatterer to a receiver at a range $R_r$ at an angle in the [*x,y*] plane of $\phi$ clockwise from the negative *x* axis may be similarly expanded yielding the approximate Green function

$$G\left(R_r,z,z_{scat},X\left(y\right),y\right)\simeq C_r\sum_{m=1}^{N}\frac{\phi_m\left(z_{scat}\right)\phi_m\left(z\right)}{\sqrt{k_m}}\exp\left(ik_m\left(\begin{array}{l}R_r+\cos\phi\left(\frac{\partial X\left(y\right)}{\partial y}y+\frac{1}{2}\frac{\partial^2 X\left(y\right)}{\partial y^2}y^2\right)-\sin\phi\left(y\right)\\+\frac{\left(\left(1-\sin^2\phi\right)+2\cos\phi\sin\phi\frac{\partial X\left(y\right)}{\partial y}+\left(1-\cos^2\phi\right)\left(\frac{\partial X\left(y\right)}{\partial y}\right)^2\right)y^2}{2R_r}\end{array}\right)\right)$$

where

$$C_r = e^{i\pi/4} / \rho(z_{scat}) \sqrt{8\pi R_r} \, .$$

The scattered field at the receiver is then found from Green's theorem as (Pierce, 1981)

$$p_{scat}(R_r) \simeq \frac{1}{4\pi} \int_0^\infty dz \int_{-\infty}^\infty dy \left( p_{scat}(z, X(y)) \frac{\partial G(R_r, z, X(y), y)}{\partial n(y)} - G(R_r, z, X(y), y) \frac{\partial p_{scat}(z, X(y), y)}{\partial n(y)} \right),$$

which may be evaluated by the method of stationary phase and by utilizing the orthogonal properties of normal modes. Furthermore, the time domain scattered field may also be obtained by utilizing time-domain extensions of the above equation.

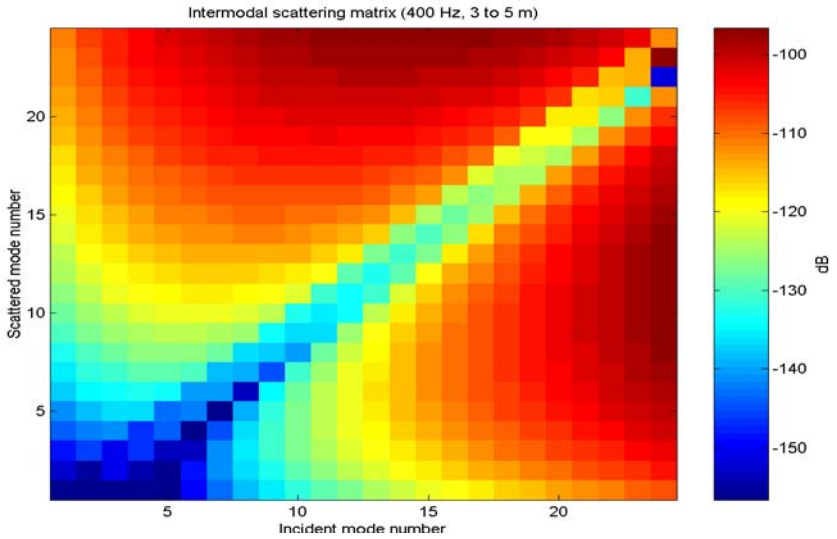


**Figure 34: Backscattered transition matrix $T_{nm}$ for a step change in sandy sediment thickness from 3 to 5 m in a 140 m deep shallow water waveguide at 400 Hz.**

We provide an example of a time domain calculation of bistatic scattering from various extended sub-bottom structures. In all cases the scenario is scattering from a step change in sediment thickness in a canonical New Jersey Strataform shallow water site. The water column is 140 m deep with a sound speed of 1478 m/s. This lies over a fast sandy sediment with a sound speed of 1726 m/s, a density of 1.75 gm/cm$^3$ and an attenuation of 0.1 dB/λ. The basement has a sound speed of 2300 m/s, a density of 2.1 gm/cm$^3$ and an attenuation of 0.5 dB/λ. The sediment thickness changes from 3 m to 5 m at a sudden discontinuity in range. The resulting backscatter transition matrix $T_{nm}$ is shown in Figure 34.

The first example is monostatic backscattering from the step change in sediment thickness at a constant range of 10 km from a monostatic source/receiver pair. The prediction of the backscatter from this feature is shown georeferenced onto the [*x,y*] plane in Figure 35 (the scatterer trajectory is shown by the thin red line.) A background sound speed of 1478 m/s was used to map the time-angle backscatter to the spatial domain. The result shows significant time spread in the coherent reflection when mapped to the spatial domain, with returns shown over a 2 km band of bottom, all at ranges greater than the actual range of the discontinuity. Indeed in this

shallow water environment there are 60 trapped modes at 400 Hz, and the group speed of the highest order modes is approximately 1000 m/s, yielding georeferenced range errors as great as 50% for returns associated with higher order excitation and scattering from the bottom discontinuity.

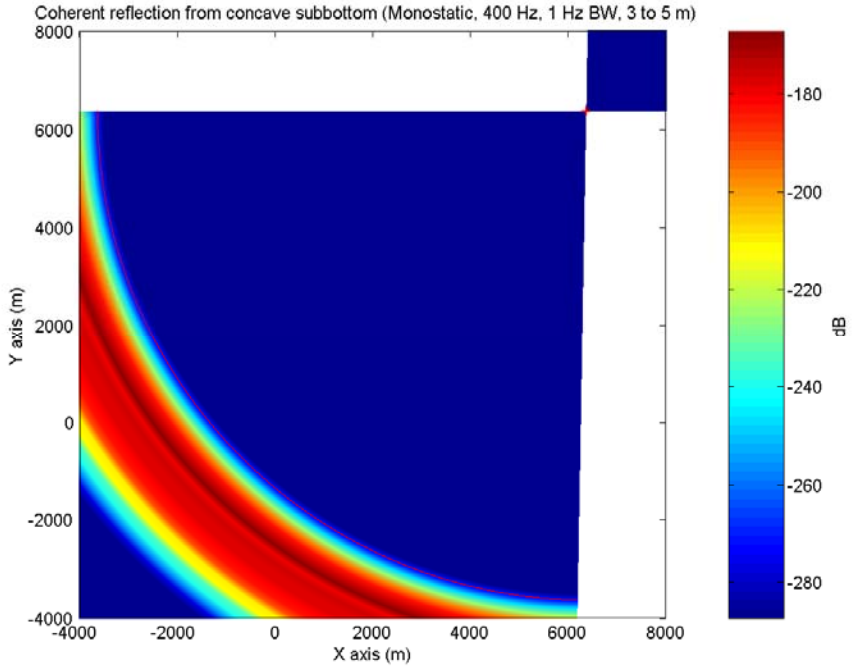


**Figure 35: Backscattered field at 400 Hz from a concave step change in sediment thickness with a radius of curvature of 10 km, monostatically ensonified and measured at the radius foci.**

The second example is monostatic backscattering from the same feature imaged from the opposite side, shown in Figure 36. Here a glint is observed at the point where the scatterer trajectory (shown in red) is perpendicular to the direction vector pointing towards the source/receiver pair. Note also that the return is approximately 15 dB lower than in the concave scattering case, due to the longer range (6 dB,) and fact that backscatter from the convex feature is destructively interfering over the receiver aperture (here 1° at 10 km or approximately 175 m, at the extremes of which the round trip phase has accumulated an extra 5 radians).

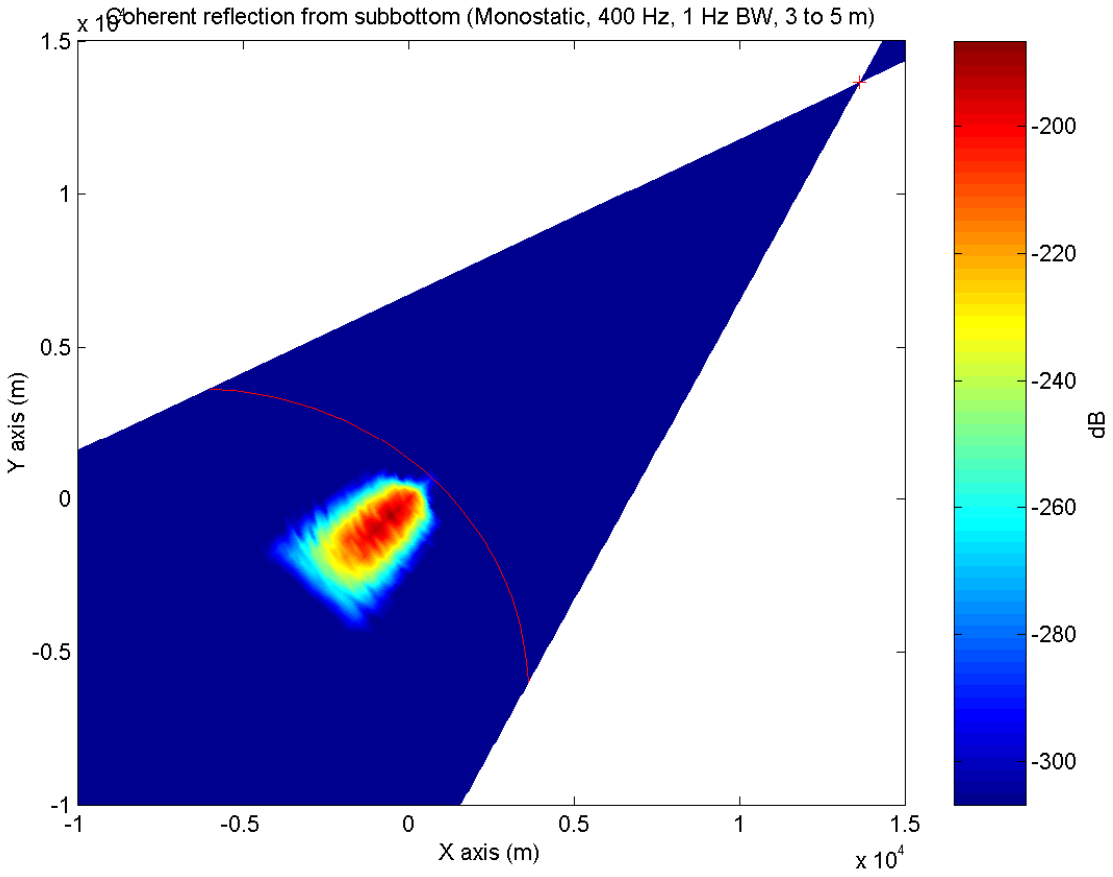


**Figure 36: Backscattered glint at 400 Hz from a convex step change in sediment thickness with a radius of curvature of 10 km, monostatically ensonified and measured at a range of 20 km from the nearest approach.**

Finally, we illustrate a bistatic result for the same convex scatterer in Figure 37. Here the receiver has been moved laterally 11.6 km to the west (left.) The specular point has moved to the point along the trajectory where the direction vectors to the source and receiver are mirror pairs about the scatterer trajectory normal. Note that the peak level is actually a few dB higher due to the reduced transmission loss. The specular point also migrates to the east for the later arrivals, an artifact of incorrect registration of the time domain returns to the georeferenced display. The actual equal travel time ellipses for the later arriving modes should be tangent to the scatterer trajectory at the indicated angle from the receiver. If the arrivals were registered with the correct travel times then the returns would all be mapped to the specular point on the scatterer trajectory.

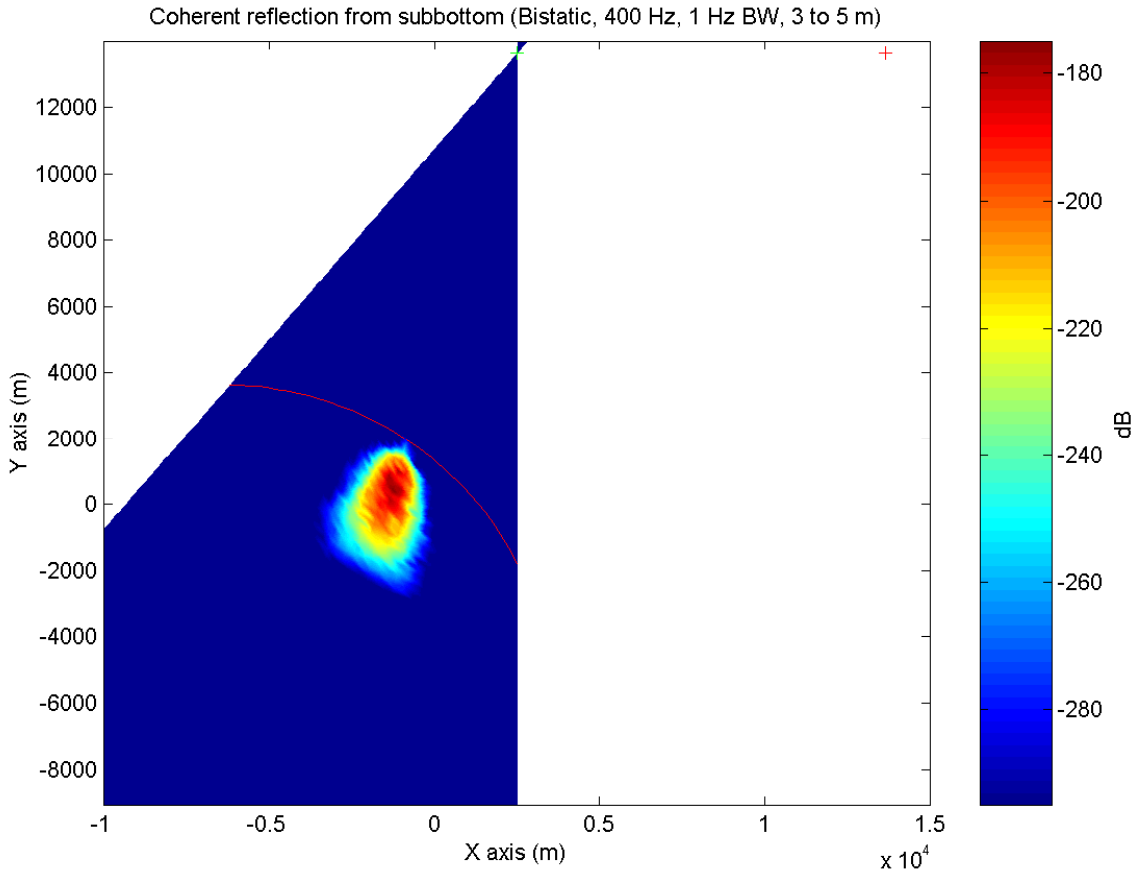


**Figure 37: Backscattered glint at 400 Hz from a convex step change in sediment thickness with a radius of curvature of 10 km, bistatically ensonified from a range of 20 km from the nearest approach and received 11.6 km to the west.**

### Summary of Phase I Findings

The phase I findings illustrate both the depth of the current understanding of the physical mechanisms that cause discrete clutter for active ASW sonar systems and the ability to simulate broadband discrete clutter time series. The results showing the target-like returns from mud volcanoes in the Malta Plateau illustrate both the degree to which the physical mechanisms behind geoclutter are understood and the likelihood that many other mechanisms are not even known, like mud volcanoes were just a few years ago. As has been stated at the outset of this work, only a subset of mechanisms responsible for target-like clutter are currently known and a subset of those mechanisms known are understood to the degree that they can be modeled.

The survey of the current reverberation model reveals that the two Navy standard performance prediction models, ASPM and CASS, each are unsuitable candidates for a starting point for the Phase II work. SST is a very capable simulation package but is unfortunately tailored for the high-frequency community with its use of the GRAB eigenray propagation loss model. As the

lead developer of SST noted, "Farther reaching changes would extend SST's applicability down to lower frequencies. A bottom model with penetration to sub-bottom layers would be a good start. A more radical change would be to incorporate some form of Parabolic Equation (PE) or other wave-based propagation model." Conversations with Robert Goddard, developer of SST, lead to the conclusion that the task of modifying SST for low-frequency simulations would be larger in size than could be done under the scope of the Phase II funding.

The research by Chris Harrison and Kevin LePage each present some unique capabilities for computing diffuse reverberation. As Kevin LePage noted in his evaluation of Harrison's work, "Recently Chris Harrison has derived complimentary analytic predictions of diffuse reverberation for bistatic scenarios in range dependent environments with either isovelocity or constant sound speed gradients. The power of this predictive capability cannot be overestimated. The reverberation predictions are very fast and agree closely with more laboriously obtained predictions." This path present the option of creating a very fast predictive capability using the analytic formulae of Harrison and the statistical distribution of the reverberation time series developed by Lyons, Abraham and others. The SUPREMO tool developed at SACLANTCEN by Chris Harrison and others also presents another option with some modifications necessary for the extension of the predictions to a time series. However, the model approach developed by Kevin LePage during his time at SACLANTCEN and NRL-DC are suitable to the problem of directly modeling reverberation time series in the low to mid frequency range.

The approach developed by Kevin LePage covered in this section of the report relies on the fact that normal mode methods are directly applicable for predicting time series in narrow bands (approximately one tenth of the center frequency) to efficiently predict reverberation from arbitrary distributions (realizations) of scatterers. This approach, initially developed for range-independent environments and monostatic geometries, has been extended to range dependent environments and bistatic geometries for reverberation intensity. The extension to bistatic geometries and more general environments is expected to be a relatively straightforward process. With the results to date and the expansion of its capabilities to handle a broader variety of simulation problems, the modeling approach developed by Kevin LePage is recommended for further development in the Phase I option and the Phase II plan.

## Phase II Tasks (Estimate of Technical Feasibility)

With a recommendation made for the modeling approach to be further developed under the Phase I option and the Phase II plan, the future tasks can now be defined more clearly than at the start of the Phase I tasks. The Phase I option to be carried out over three months[12] following the completion of the Phase I base program will work to identify in-water data sets for testing of the model during the Phase II tasking, identify the interface requirements for the use of the Phase II simulation by the EER and LAMP program, begin work on the documentation for the simulation and begin the work on modifying the current model from Kevin LePage to satisfy the requirements of the simulation.

[12] Email from John Williams (Navy STTR Program Manager) on 16 January 2004 states Phase I options to begin on 1 May 2004 for those Phase II proposals selected for award.

The proposed Phase II tasking will allow the model development conducted to date through the Phase I base program and the Phase I option program to be developed into a mature, configuration managed modeling product. The Phase II tasks include the continuation of the acoustic data analyses by Charles Holland at ARL/PSU for the development of additional understanding and modeling for various geoclutter mechanisms. Additional task will include the additional model development at NRL-DC by Kevin LePage and specifically the implementation of the modeling for the identified geoclutter mechanisms from Charles Holland. The acoustic data sets identified for model-to-data comparison by ARL/PSU will be used to provide feedback to NRL-DC for additional model upgrades and will be used as an initial report for either OAML approval or for an independent V&V evaluation of the model. A final task for the Phase II base program will be to produce a configuration managed version of the model (still within Matlab) with corresponding documentation. The Phase II option program is designed to produce upgraded versions of the model to satisfy particular program needs. The ability to model the frequency spread due to interaction with the sea-surface and the ability to provide beamformed output for the EER family of sensors are both tasks proposed for the Phase II option program.

**Phase I Option**

The Phase I Option Program consists of three tasks building on the results of the Phase I Base Program. The first task identifies key in-water reverberation data sets that will be used for Phase II model development and begins the process of transitioning the identified clutter mechanisms from Base Program Task 1 into the reverberation model developed by Kevin LePage. The second task begins the transition of the Kevin LePage's model into configuration managed form. With a projected transition of the broadband model developed under this Phase II STTR to the AEER program, the model will be maintained in MATLAB. The goals of this task is to define the needs of the AEER program in terms of interfaces to their current signal processing algorithm and performance prediction algorithm currently written in MATLAB. An outline of the documentation for the broadband time series model will also be generated under this task. The third task includes the integration of the diffuse reverberation and discrete clutter modeling approaches selected and identified in the Phase I Base Program into the Kevin LePage's model.

***Option Program Task 1 –Identification of Key in-water data sets for Phase II model evaluation/development and Model Implementation of Selected Clutter Mechanisms***

Under the Phase I Option Program Task 1, key in-water data sets will be identified that will be used under the Phase II model evaluation/development effort. Criteria for selecting the data sets include: measured reverberation time series with a significant clutter feature; supporting environmental data including bathymetry; water column as well as seabed scattering and reflection data. Local (close-range) scattering from the clutter event is also highly desirable and may be available for some runs. We will want to select several data sets, in differing environments, with differing clutter features. The data sets from AEER, MACE and ALFEA that were discussed with the EER and LAMP program representatives will also be included in the data sets considered. The physical mechanisms identified by ARL/PSU in Phase I Base Program Task 1 will begin to be explicitly modeled in a form compatible with the chosen approach for modeling diffuse reverberation from the Phase I Base Program.

*Products from Option Program Task 1*

Under this Option Program task, ARL/PSU will identify key data sets containing measured reverberation plus scattering and reflection (and geoacoustics) that can be used in Phase II to exercise, develop and refine the physics-based diffuse reverberation and discrete clutter model. ARL/PSU will also provide expert knowledge to NRL-DC to guide the model implementation of the clutter mechanisms.

*Timetable and Costing for Option Program Task 1*

The work on option program task 1 will be conducted over a 3 month period of performance following the Phase I Base Program. Charles Holland of ARL/PSU will be the lead investigator on this task with all work on this task done at ARL/PSU.

The proposed costing for the Phase I option program task 1 is $15,000 for ARL/PSU as a subcontractor to PSI. This costing includes labor, overhead, G&A expense and travel.

***Option Program Task 2 –Configuration Management of Selected Modeling Approach***

Under the Phase I Option Program task 2, Peter Neumann and Gregory Muncill of PSI will work with representatives of both the AEER and LAMP programs to determine their exact needs to interface the broadband time series model to be developed. The model will be written and delivered in MATLAB which is preferable to the AEER program. It is important prior to beginning the Phase II tasking that the software design is documented so that all participants know the design goals of the work. The second task that will be addressed at this time will be an outline for the model documentation that provides detailed information on all inputs and outputs. As funding permits during the task, this outline will be flushed out with details on the model under development. In a conversation with the AEER program representatives, it was also discussed that their use of this model would be helped by an OAML approval or an independent V&V (validation and verification) of the model at the end of the Phase II development. The potential for either of these would also be investigated under this task through conversations with the OAML chairman and other V&V efforts for models and algorithms.

*Products from Option Program Task 2*

Under this Option Program task, PSI will work with the AEER program and the LAMP program to determine their specific needs for interfacing the broadband time series model into their current signal processing and system performance algorithms written in MATLAB. The results of this work will be a design document for the broadband time series model that specifies all inputs (environmental, source, and receiver) and outputs (raw time series, beam formed time series, etc.). An outline for the model documentation will also be generated and some initial work on that documentation will be done as funding permits. The options for OAML submission or a V&V of the model will also be investigated and reported.

*Timetable and Costing for Option Program Task 2*

The work on option program task 2 will be conducted over a 3 month period of performance following the Phase I Base Program. Peter Neumann of PSI will be the lead on this task working with Gregory Muncill of PSI with work being done at the PSI locations in Blacksburg, VA; Silver Spring, MD; and Reston, VA.

The proposed costing for the Phase I option program task 2 is $14,980 which includes labor, overhead, G&A expense and travel.

***Option Program Task 3 – NRL-DC Model Implementation of Selected Diffuse Reverberation and Discrete Clutter Models***

Under the Phase I Option Program task 3, Kevin LePage as an outside resource will begin to implement the selected aspects of the diffuse reverberation and discrete clutter models into his R-SNAP and BiStaR models. The details of this implementation will be based upon the results of the survey work on existing models for both diffuse reverberation and discrete clutter completed under the Phase I Base Program task 2.

*Products from Option Program Task 3*

The products from this task will be updated versions of the R-SNAP and BiStaR models reflecting those modeling elements that can be integrated during the period of performance of this option task.

*Timetable and Costing for Option Program Task 3*

The work on option program task 3 will be conducted over a 3 month period of performance following the Phase I Base Program. Kevin LePage of NRL-DC will be the lead investigator for this task with work being done at NRL-DC.

As an outside resource, Kevin LePage's time is being provided through the NRL Multistatics Active System Performance exploratory research initiative managed by Roger Gauss.

**Phase II Base Program**

The proposed Phase II base program is designed to deliver a complete simulation capability for a select group of discrete clutter mechanisms and for the diffuse reverberation problem. The simulation will generate broadband time series using the approach developed by Kevin LePage using a coherent summation of narrowband results. The Phase II base program is divided into four tasks. The continued work by Charles Holland on modeling discrete clutter mechanisms comprises task 1. The work by Kevin LePage on expanding the capabilities of his modeling approach is task 2. The testing and validation of the model on in-situ data sets will be done under task 3. The transition of the research model developed under task 2 into a simulation product with documentation, test cases and standard interfaces with the simulation packages of the AEER and LAMP program will comprise task 3. Additional details on each task are provided in the following sections of this report.

***Phase II Base Program – Task 1 – Model Additional Mechanisms Responsible for Discrete, Target-Like Clutter Returns in the Littoral Environment***

Analysis of two clutter events in the 1998 reverberation data set conducted yielded very valuable information about the clutter mechanisms (scattering from sediment-entrained gas and scattering from gas plumes in the water column) and their spectral and temporal characteristics. That data set exhibited a number of other clutter features that were not analyzed. These data, coupled with data from 2000 and 2002 (that have yet to be analyzed) provide a rich observational set from which to characterize additional clutter mechanisms. It will be crucial to analyze all of the significant clutter mechanisms in order to provide the development of model with as much realism as possible.

*Products from Phase II Base Program Task 1*

Charles Holland will transition knowledge about the clutter mechanisms and their characteristics to PSI and NRL during the entire course of Phase II study so that as soon as the clutter mechanisms are characterized they can be incorporated into the modeling. We expect that this will be something of an iterative process, inasmuch as initial characterizations of the clutter mechanisms may or may not be suitable to direct treatment in the model. Alternate characterizations will be explored that capture both the essence of the physical mechanism and are amenable to the modeling approach. ARL-PSU will deliver to PSI a summary report containing the significant clutter features discovered during the tasking, and the recommended method for characterization.

*Timetable and Costing for Phase II Base Program Task 1*

The work on the Phase II base program task 1 will be conducted over the 24 month period of performance of the Phase II base program. Charles Holland of ARL/PSU will be the lead investigator for this task with all work on this task done at ARL/PSU.

The proposed costing for the Phase II base program task 1 is $124,000 for ARL/PSU as a subcontractor to PSI. This costing includes labor including overhead and G&A ($105,000), hardware and software upgrades ($7,000), travel ($7,000) and subcontract administrative fee ($5,000).

***Phase II Base Program – Task 2 – Further Development on the Modeling Approach for Diffuse Reverberation and Discrete Clutter to Satisfy Simulation Requirements***

Under the Phase II base program task 2, Kevin LePage as an outside resource will be responsible for the continued development of his broadband discrete clutter and diffuse reverberation modeling. In conjunction with Charles Holland (ARL/PSU), Kevin LePage will implement the modeling for the discrete clutter mechanisms identified by Dr. Holland within the framework defined in this report. Kevin LePage will also serve as an outside expert on the model-to-data comparisons conducted during the Phase II base program task 3. Feedback from the model-to-data comparisons will provided to Kevin LePage during the entire Phase II base program period of performance.

*Products from Phase II Base Program Task 2*

The product of this task is a Matlab based broadband time series simulation for both diffuse reverberation and the discrete clutter mechanisms that have been identified and modeled as part of this STTR. The code is Matlab will be provided incrementally to PSI for both model-to-data comparisons and for inclusion in the final configuration managed deliverable.

*Timetable and Costing for Phase II Base Program Task 2*

The work on the Phase II base program task 2 will be conducted over the 24 month period of performance of the Phase II Base Program. Kevin LePage of NRL-DC will be the lead investigator for this task with work being done at NRL-DC.

As an outside resource, Kevin LePage's time is being provided through the NRL Multistatics Active System Performance exploratory research initiative managed by Roger Gauss.

***Phase II Base Program – Task 3 – Rigorous Model-to-Data Comparisons using Reverberation Data and Concomitant Environmental Characterization***

A frequently insurmountable problem in comparing a reverberation model against measurements (even for diffuse reverberation) is having sufficient control over the inputs. Diffuse reverberation decay depends on many environmental factors including bathymetric, water column, and (often dominated by) seabed forward reflection and scattering strength variability. Without knowing each of those components a model-to-data comparison may simply become an exercise in turning knobs. For example, reverberation decay depends upon both bottom reflection loss and scattering in ways that are often indistinguishable so that without independent measurements of those quantities a meaningful model evaluation is impossible.

Model-to-data comparisons for clutter are even more complex. It is not only necessary to have controls on the seabed reflection (controlling forward propagation) and seabed scattering (controlling the diffuse reverberation near the clutter event) but high-resolution geoacoustic information at and near the clutter site and spatial and geoacoustic characteristics of the geoclutter feature are also required. The geoacoustic properties at the clutter feature are particularly important when the clutter feature is buried beneath the seafloor; that is, the modeling must properly account for the transmission across the water sediment interface, attenuation through the medium, transmission across any layer boundaries in the medium, scattering from the geoclutter feature and then transmission back into the water column. ARL-PSU has several data sets that have extensive measurements of seabed reflection and scattering in the northern Tyrrhenian Sea, the Straits of Sicily (Malta Plateau) and the New Jersey Shelf, for the explicit purpose of providing such controls. In addition to the reflection and scattering measurements mentioned above, we have also conducted close-range measurements of clutter characteristics and high-resolution seabed geoacoustic properties that will be crucial for evaluating and development of the model. We believe that our team (ARL/PSU, NRL-DC and PSI) has a unique capability in this arena to provide meaningful model-to-data analyses.

In this task, ARL-PSU will analyze the acoustic data to provide the required geoacoustic inputs to the reverberation model. These inputs would include, for example, the range dependent meso-

scale geoacoustic model that controls forward propagation, the fine-scale geoacoustics, that control the diffuse reverberation and the feature-based geoacoustics that control scattering from the clutter object.

With acoustic data and supporting environmental data provided by ARL/PSU, both PSI and NRL-DC will perform model-to-data comparisons to investigate the ability of the simulation to replicate the observed acoustic data. The feedback from the comparisons will be provided to NRL-DC and further refinement of the model (Phase II base program task 2). Model-to-data comparisons will include both basic comparisons for the diffuse reverberation modeling and statistical measures of the time series for both discrete clutter and diffuse reverberation.

*Products from Phase II Base Program Task 3*

The product from the Phase II base program task 3 will be a report summarizing the model-to-data comparisons. This report will include the work performed by ARL/PSU during which the selected acoustic data sets (Phase I option program task 1) have been analyzed for the required geoacoustic input parameters. The results of the model-to-data comparisons performed by PSI will be included along with the resulting feedback to NRL-DC and any changes to the modeling made as a result of the comparison results.

*Timetable and Costing for Phase II Base Program Task 3*

The work on the Phase II base program task 3 will be conducted over the 24 month period of performance of the Phase II Base Program. Peter Neumann of PSI will be the lead investigator for this task with work on this task being done by key personnel from ARL/PSU, NRL-DC and PSI.

The proposed costing for the Phase II base program task 3 is $241,000 including $116,000 for ARL/PSU as a subcontractor to PSI and $125,000 for PSI. The costing for ARL/PSU includes labor ($103,000), hardware and software upgrades ($6,000) and travel ($7,000). The costing for PSI includes labor ($108,000), hardware and software upgrades ($8,000), travel ($4,000) and subcontract administrative fee ($5,000). Software for PSI includes two licenses for Matlab including the signal processing toolbox and the annual software maintenance service for the second year of the task.

***Phase II Base Program – Task 4 – Configuration Management and Documentation of Modeling Approach for Use in Existing and Future Active Sonar Simulators***

The Phase II base program task 4 will transform the Matlab modeling code provided by Kevin LePage (Phase II base program task 2) into a configuration managed model for use by those programs identified during the Phase I and Phase II period of performance. The configuration management will include writing the required software interfaces to connect the model with the simulations in use by the various programs. This task will provide complete documentation for the model in a format similar to (if not identical to that) required by OAML. Under Phase I option program task 2 PSI will explore the options for OAML approval or an independent V&V

of the model as requested by the AEER program during the meeting on December 11th, 2003. The results of the option program task will direct the format for the documentation of the model.

*Products from Phase II Base Program Task 4*

The products from Phase II base program task 4 will be a configuration managed version of the modeling software in Matlab format with supporting documentation. If it is determined that the model will be submitted for OAML approval, that documentation will adhere to the OAML documentation standards that PSI has written to for various other models and databases. If it is determined that the model will not submitted for OAML approval, the format of the documentation will be determined in consultation with the potential end-users.

*Timetable and Costing for Phase II Base Program Task 4*

The work on the Phase II base program task 4 will be conducted over the 24 month period of performance of the Phase II Base Program. Peter Neumann of PSI will be the lead investigator for this task with work being done at PSI.

The proposed costing for the Phase II base program task 4 is $135,000 for PSI. The costing for PSI includes labor ($129,000), hardware and software upgrades ($2,000) and travel ($4,000).

**Phase II Option Program**

The two Phase II option tasks presented satisfy particular requirements of the AEER program. In the meeting with the representatives of the AEER program on December 11th, 2003, two requirements of the broadband time series simulation were stated that were not in the initial plans as defined in the Phase I proposal. Task 1 will add the ability to model the frequency spread due to interaction with the sea surface. This capability was not proposed in the initial Phase I proposal but is clearly an important effect that must be modeled for the AEER program to consider using the model. The second task is a much smaller task that would add the ability to do the beamforming for sensors specific to the AEER program. Each of these tasks would add greatly to the capability of the model and would address specific needs from a program that is interested in the potential use of the model.

***Phase II Option Program – Task 1 – Modeling of Frequency Spread due to Surface Scattering***

Under the Phase II option program task 1 the ability to model the frequency spread resulting from the interaction with the air-water interface and the near-surface bubble clouds will be added to the model developed under the Phase II base program. The approach does not look to conduct basic research on this effect but looks to transition the results developed to date (including those from NRL-DC, Gragg, 2003) into the model. There is an internal funding proposal within NRL-DC for research into this effect that would start in FY 05. If this task were exercised near or at the completion of the Phase II period of performance, the results from this research at NRL-DC could also be leveraged into the model.

*Products from Phase II Option Program Task 1*

The product from the Phase II option program task 1 would be a modified version of the model developed under the Phase II base program with the added capability of including the frequency spread in the received signal caused by interaction with the air-water interface and the near surface bubble clouds. The changes to the model would also be reflected in an updated set of documentation following the same format of the documentation created under the Phase II base program task 4.

*Timetable and Costing for Phase II Option Program Task 1*

The timetable for the Phase II option program task 1 would be a period of performance of 12 months starting near or at the completion of the Phase II base program period of performance. Peter Neumann of PSI will be the lead investigator for this task with work being done at PSI in conjunction with experts in the field at NRL-DC and within the AEER program.

The proposed costing for the Phase II option program task 1 is $200,000 for PSI. The costing for PSI includes labor ($194,000), hardware and software upgrades ($2,000) and travel ($4,000).

***Phase II Option Program – Task 2 – Integration of Beamforming Algorithms Specific to NAVAIR's EER Program***

Under the Phase II option program task 2 the ability to provide beamformed output for the various sensors in the EER program would be added to the model developed under the Phase II base program. This task represents a small effort but would add a capability that is of great value to the AEER program. The beamforming routines necessary for the EER sensors would be added to the configuration managed model in a manner consistent with the requirements of the AEER program.

*Products from Phase II Option Program Task 2*

The product for the Phase II option program task 2 would be a modified version of the model developed under the Phase II base program with the added capability to provide beamformed output for EER specific sensors. The additions to the model necessary for this task would also be reflected in an updated set of documentation following the same format of the documentation created under the Phase II base program task 4.

*Timetable and Costing for Phase II Option Program Task 2*

The timetable for the Phase II option program task 1 would be a period of performance of 3 to 6 months starting near or at the completion of the Phase II base program period of performance. Peter Neumann of PSI will be the lead investigator for this task with work being done at PSI in conjunction with experts in the field from the AEER program.

The proposed costing for the Phase II option program task 2 is $50,000 for PSI. The costing for PSI includes labor ($46,000), hardware and software upgrades ($2,000) and travel ($2,000).

## Phase III Commercialization Opportunities

During the Phase I base program, two potential transitions for the simulation proposed for development under the Phase II work plan were identified. In a meeting with Rick Fillhart of the EER program and Dave Fenton of the LAMP program, the utility of this type of simulation product was evident if the simulation could satisfy their specific program's requirements. The proposed Phase II tasks and specifically the Phase II option tasks address some specific requirements of the AEER program that were brought out during that meeting. The proposed simulation tool, capable of producing realistic, broadband time series prediction for environments including the effect of target-like clutter from a select group of physically understood mechanisms would be a valuable tool for use in active sonar system design. The ability to accurately simulate broadband time series for a hypothetical source/receiver before doing in-water testing should allow for a more cost effective design and allow the in-water testing that is done on more mature designs.

## Acknowledgements

The authors of this report would like to thank the many developers of the models discussed in this report for their help and contributions to this report. Tony Eller of SAIC has graciously provided the latest version of ASPM 5.1 along with the supporting documentation and the PowerPoint presentation from which the examples outputs from ASPM were taken. Robert Goddard of APL/UW provided us with SST 4.1 and SST 4.2 as well as all the documentation noted in the reference section of this report for SST. Mr. Goddard met with Peter Neumann and Greg Muncill at PSI on October 27th and provided a great many details on SST as well as a demonstration of SST running on his laptop using Cygwin under Windows. Chris Harrison graciously provided copies of the SACLANTCEN reports cited in this report for his reverberation modeling work.

The authors would also be remiss if they did not thank Roger Gauss of NRL-DC without whose assistance the time and efforts of Kevin LePage would not be available for the work on this STTR. The expertise of Kevin LePage and the other modelers at NRL-DC has added greatly to the scope and capabilities of the discrete clutter and diffuse reverberation modeling effort undertaken.

## References Cited in the Report

Abraham, D. A. and A. P. Lyons, "Novel physical interpretations of K-distributed reverberation," *IEEE Journal of Oceanic Engineering*, **27** (4) 800-813 (2003).

Baldacci, A. and Harrison, C.H., SUPREMO Version 1.0 Users Guide, SACLANTCEN M-141 (2002).

Bouchage, G. and K. D. LePage, "A shallow water reverberation PE model," *Acta Acustica*, **88** (5), 638-641 (2002).

Dosso, S. E. and C. W. Holland, "Bayesian geoacoustic inversion of seabed reflection data," *Journal of the Acoustical Society of America*, in review.

Duckworth, G., K. LePage and T. Farrell, "Low frequency long range propagation and reverberation in the central Arctic: Analysis of experimental results," *Journal of the Acoustic Society of America*, **110** (2), 747-760 (2001).

Ferla, C. M., M. B. Porter, and F. B. Jensen, *C-SNAP: Coupled SACLANTCEN normal mode propagation model*, SACLANT Undersea Research Centre SM-274, La Spezia, Italy (1993).

Fialkowski, J., R. C. Gauss and C. D. Drumheller, "Measurements and Modeling of Low-Frequency Surface Scattering Statistics," *IEEE Journal of Oceanic Engineering*, in press (2004).

Gauss, R. C. and J. M. Fialkowski, "A Broadband Model for Predicting Bistatic Surface Scattering Strengths," in *Proceedings of the Fifth European Conference on Underwater Acoustics*, ed. by M. E. Zakharia et al., (European Commission, Luxembourg), Vol. 2, pp. 1165-1170 (2000).

Gilbert, K. E., "A stochastic model for scattering from the near-surface oceanic bubble layer," *Journal of the Acoustical Society of America*, **94** (6), 3325-3334 (1993).

Goddard, R. P., "The Sonar Simulation Toolset," submitted for publication in the *U.S. Navy Journal of Underwater Acoustics* on August 28, 2003.

Goddard, R. P., "The Sonar Simulation Toolset Web, Release 4.1," APL-UW TM 10-96 (Electronic Document), Revised 2002, Applied Physics Laboratory, University of Washington, Seattle, WA (November 2002).

Goddard, R. P., "Sonar Simulation Toolset, Release 4.0," PowerPoint presentation provided by Robert P. Goddard (APL/UW) (January 2002).

Goddard, R. P., "SST Bistatic Reverberation Modeling: North Sea Experiment, April-May 1998," APL-UW TM 5-00, Applied Physics Laboratory, University of Washington, Seattle, WA (May 2000).

Goddard, R. P., "The Sonar Simulation Toolset," *Proceedings Oceans '89, The Global Ocean*, Volume 4, 1217-1222 (1989).

Gragg, R. F., "Doppler sidebands in the cross-spectral density of narrow-band reverberation from a dynamic sea surface," *Journal of the Acoustical Society of America*, **114** (3), 1387-1394 (2003).

Harrison, C. H., "Closed-form expressions for ocean reverberation and signal excess with mode stripping and Lambert's law," *Journal of the Acoustic Society of America*, **114** (5), 2744-2756 (2003).

Harrison, C. H., *Formulae for Signal Reverberation with Variable Bathymetry and Refraction*, SACLANTCEN SR-358 (2003).

Harrison, C. H., *Formulae for Bistatic Signal and Reverberation*, SACLANTCEN SR-371 (2002).

Harrison, C. H., *Signal and Reverberation Formulae Including Refraction*, SACLANTCEN SR-370 (2002).

Harrison, C. H., *Signal and Reverberation with Mode-stripping and Lambert's Law*, SACLANTCEN SR-356 (2002).

Holland, C.W., T. C. Weber and P. Boni, "Acoustic remote sensing of gassy sediments and gas flux from submarine mud volcanoes," *Journal of the Acoustical Society of America,* (in review).

Holland, C. W., G. Etiope, A. V. Milkov, E. Michelozzi and P. Favali, "Mud volcanoes discovered offshore Sicily," *Marine Geology*, **199**, 1-6 (2003).

Holland, C.W., "Shallow water coupled scattering and reflection measurements," *IEEE Journal of Oceanic Engineering*, **27**, 454-470 (2002).

Holland, C.W. and P. Neumann, "Sub-bottom scattering; A modeling approach," *Journal of the Acoustical Society of America*, **104** (3), 1363-1373 (1998).

Holland, C. W., P. M. Ogden, M. T. Sundvik, and R. Dicus, "Critical Sea Test Bottom Interaction Overview," SPAWAR CST/LLFA-WP-EVA-46 (September 1996).

Jackson, D. R. and K. B. Briggs, "High-frequency bottom backscattering: Roughness versus sediment volume scattering," *Journal of the Acoustical Society of America*, **92** (2), 962-977 (1992).

Jackson, D. R., D. P. Winebrenner and A. Ishimaru, "Application of the composite roughness model to high-frequency bottom backscattering," *Journal of the Acoustical Society of America*, **79** (5), 1410-1422 (1986).

Jensen, F. B., W. A. Kuperman, M. B. Porter, and H. Schmidt, *Computational Ocean Acoustics*, AIP press, New York (1994).

Keenan, R. E., "An Introduction to GRAB Eigenrays and CASS Reverberation and Signal Excess," *IEEE Oceans 2000*, 1065-1070 (2000).

Keenan, R. E. and H. Weinberg, "Gaussian Ray Bundle (GRAB) Model Shallow Water Acoustic Workshop Implementation," (November 1999).

Keenan, R. E., "Technical Memorandum: Broadband Bistatic Reverberation Applications of CASS," prepared for Robert Miyamoto of APL/UW (October 1999).

Kopf, A. K., "Significance of mud volcanism," *Reviews of Geophysics*, **40** (2), 1-52 (2002).

LePage, K.D., "Statistics of broadband bottom reverberation predictions in shallow water waveguides," *IEEE Journal of Oceanic Engineering*, in review.

LePage, K.D. and H. Schmidt, "Spectral integral representations of monostatic backscattering from three dimensional distributions of sediment volume inhomogeneities," *Journal of the Acoustic Society of America*, **113** (2), 789-800 (2003).

LePage, K. D., Modal travel time, dispersion and approximate time series synthesis in range dependent waveguides, *SACLANT Undersea Research Centre SR-350*, La Spezia, Italy (2002).

LePage, K. D., Modeling propagation and reverberation sensitivity to oceanographic and seabed variability, *SACLANT Undersea Research Centre SM-398*, La Spezia, Italy (2002).

LePage, K. D., Monostatic reverberation in range dependent waveguides: the R-SNAP model, *SACLANT Undersea Research Centre SR-363*, La Spezia, Italy (2002).

LePage, K. D., "Acoustic time series variability and time reversal mirror defocusing due to cumulative effects of water column variability," *Journal of Computational Acoustics,* **9** (4), 1455-1474 (2001).

LePage, K. D. and H. Schmidt, "Spectral integral representations of volume scattering in ocean waveguides," *Journal of the Acoustic Society of America*, **108** (4), 1557-1567 (2000).

LePage, K. D., "Bottom reverberation in shallow water: Coherent properties as a function of bandwidth, waveguide characteristics, and scatterer distributions," *Journal of the Acoustic Society of America*, **106** (6), 3240-3254 (1999).

Levin, J. J., W. W. Renner and A. I. Eller, "Software Design Description for the Acoustic System Performance Model," SAIC-00/1032 (June 2000).

Levin, J. J., W. W. Renner and A. I. Eller, "Software Requirements Specifications for the Acoustic System Performance Model," SAIC-99/1008 (January 1999).

Levin, J. J., W. W. Renner and A. I. Eller, "Software Test Document for the Acoustic System Performance Model," SAIC-99/1007 (January 1999).

Mackenzie, K. V., "Bottom Reverberation for 530 and 1030 cps Sound in Deep Water," *Journal of the Acoustical Society of America*, **33** (11), 1498-1504 (1961).

Makris, N. C., "Imaging ocean-basin reverberation via inversion," *Journal of the Acoustical Society of America*, **94**, 983-993 (1993).

Max, M. D., N. Portunato, and G. Murdoch, *Sub-seafloor reflectors imaged by low-frequency active sonar*, SACLANT Centre Memo, SM-306 (1996).

Max, M. D., A. Kristensen and E. Michelozzi, *Small scale Plio-Quaternary sequence stratigraphy and shallow geology of the west-central Malta Plateau*, SACLANT Centre Report, SR-209 (1993).

McDaniel, S. T., "Models for Predicting Bistatic Surface Scattering Strength," ARL-PSU TM 90-88, Applied Research Laboratory, Pennsylvania State University, State College, PA (March 1990)

Milkov, A.V., "Worldwide distribution of submarine mud volcanoes and associated gas hydrates," *Marine Geology*, 167, 29-42 (2000).

Mourad, P. D. and D. R. Jackson, "A model/data comparison for low-frequency bottom backscatter," *Journal of the Acoustical Society of America*, **94** (1), 344-358 (1993).

Neumann, P. and G. Muncill, "Software Design Description for the Low Frequency Bottom Loss Model (LFBLTAB) Version 2.4," (August 1998).

Osler J. and O. Algan, *A high resolution seismic sequence analysis of the Malta Plateau*, SACLANT Centre Report SR-311 (1999).

Pierce, A. D., *Acoustics: An Introduction to Its Physical Principles and Applications*, McGraw Hill, New York (1981).

Prior, M. K., C. H. Harrison, and K. D. LePage, *Reverberation Comparisons Between RSNAP, SUPREMO and Analytical Solutions*, SACLANTCEN SR-361 (2002).

Weinberg, H., R. L. Davenport, E. H. McCarthy and C. M. Anderson, "Comprehensive Acoustic System Simulation (CASS) Reference Guide," NUWC-NPT TM 01-016, Naval Undersea Warfare Center Division, Newport, RI (March 2001).

Weinberg, H., "CASS Roots," *IEEE Oceans 2000*, 1071-1076 (2000).

White, D., M. Bradley and B. Bradley, "Software Test Description for the ASTRAL Model (Version 5.1)," OAML-STD-23A (March 2000).

Weinberg, H. and R. E. Keenan, "Gaussian ray bundles for modeling high-frequency propagation loss under shallow-water conditions," *Journal of the Acoustical Society of America*, **100** (3), 1421-1431 (1996).

Williams, K. L. and D. R. Jackson, "Bistatic bottom scattering: Model, experiments, and model/data comparison," *Journal of the Acoustical Society of America*, **103** (1), 169-181 (1998).

Yamamoto, T., "Acoustic scattering in the ocean from velocity and density fluctuations in the sediment," *Journal of the Acoustical Society of America*, **99** (2), 866-879 (1996).

## Report Preparation

This report was prepared and submitted by the following individuals:

Peter Neumann (PSI)
(540) 552-5102 (Phone)
pneumann@plansys.com

Gregory Muncill (PSI)
(301) 565-9441 (Phone)
gmuncill@plansys.com and gmuncill@mindspring.com

Charles Holland (ARL/PSU)
(814) 865-1724 (Phone)
cwh10@psu.edu

Kevin LePage (NRL/DC)
(202) 484-4834 (Phone)
kevin.lepage@nrl.navy.mil